

Vector Boson Scattering as the gate to New Physics

Seminar at IFD UW, May 21, 2021

Michał Szleper, National Center for Nuclear Research, Warsaw

Vector Bosons and their polarizations

- **Boson wave function** $B^\mu = \epsilon^\mu e^{-i p \cdot x} = \epsilon^\mu e^{i(\vec{p} \cdot \vec{x} - E t)}$

- **Polarization vector – boson rest frame:**

$$\epsilon_x^\mu = (0, 1, 0, 0) \quad \epsilon_y^\mu = (0, 0, 1, 0) \quad \epsilon_z^\mu = (0, 0, 0, 1)$$

Lorenz condition:

$$\vec{p}_\mu \epsilon^\mu = 0$$

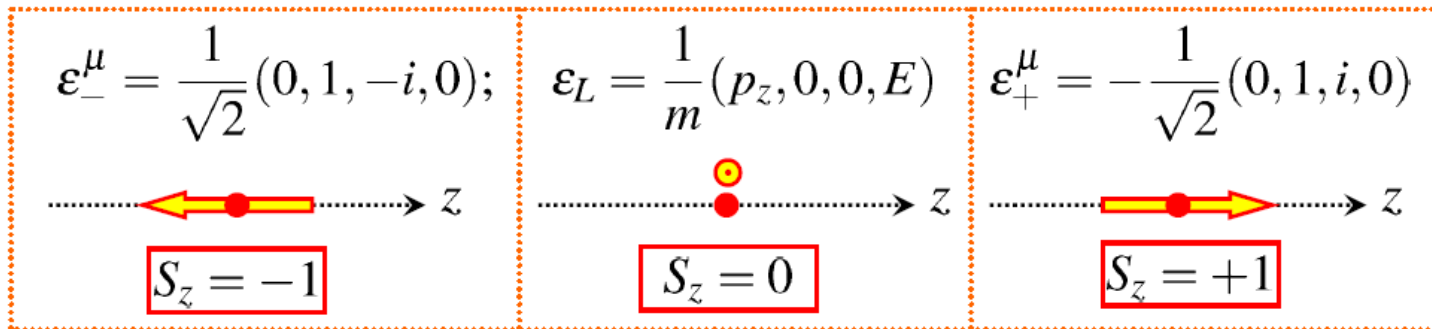
(imperative for non-zero mass)

- **Combinations of the x and y coordinates that correspond to circular polarization**

$$\epsilon_+^\mu = \frac{1}{\sqrt{2}} (0, 1, -i, 0)$$

$$\epsilon_-^\mu = \frac{1}{\sqrt{2}} (0, 1, i, 0)$$

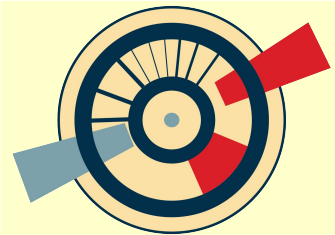
- **In the frame where the boson moves along the z axis:**



$S_z = -1, 1$ – transverse polarization (T)

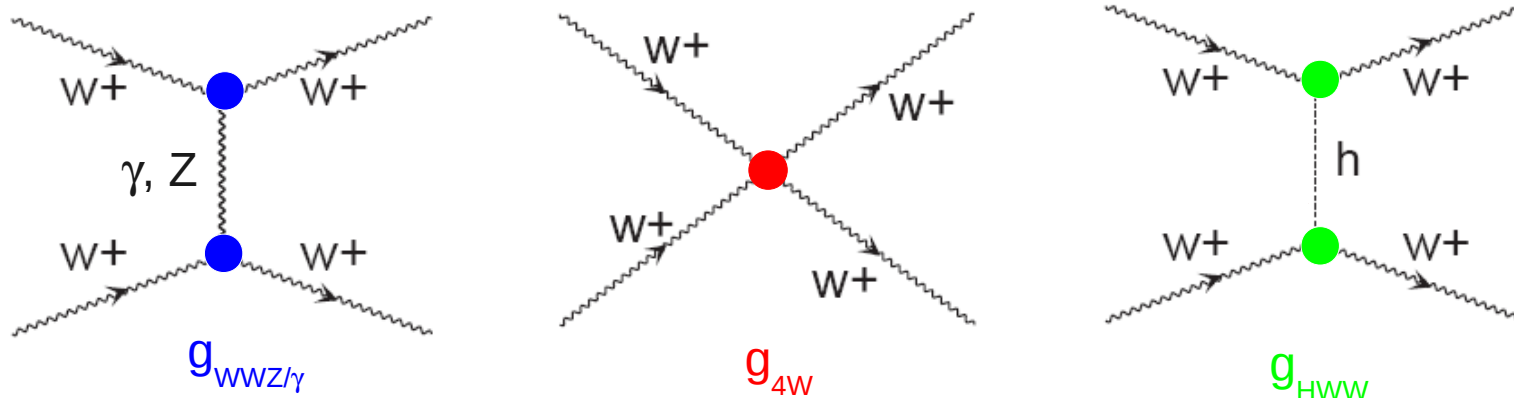
$S_z = 0$ – longitudinal polarization (L, possible only for a boson with non-zero mass)

$\epsilon_L \sim E/m$ - grows indefinitely with energy!



The physics of Vector Boson Scattering

Same-sign WW process:



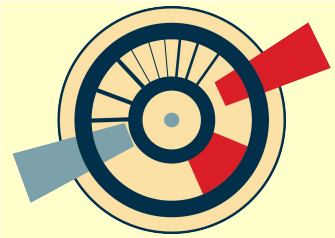
Each of these diagrams: $\mathcal{M} \sim \epsilon_L \epsilon_L \epsilon_L \epsilon_L \sim s^2$,
 by appropriate $g_{WWZ/\gamma}$ and g_{4W} setting:

$$\mathcal{M}_{gauge} = -\frac{g^2}{4M_W^2} s + \mathcal{O}(s^0)$$

With a Standard Model-like g_{HWW} :

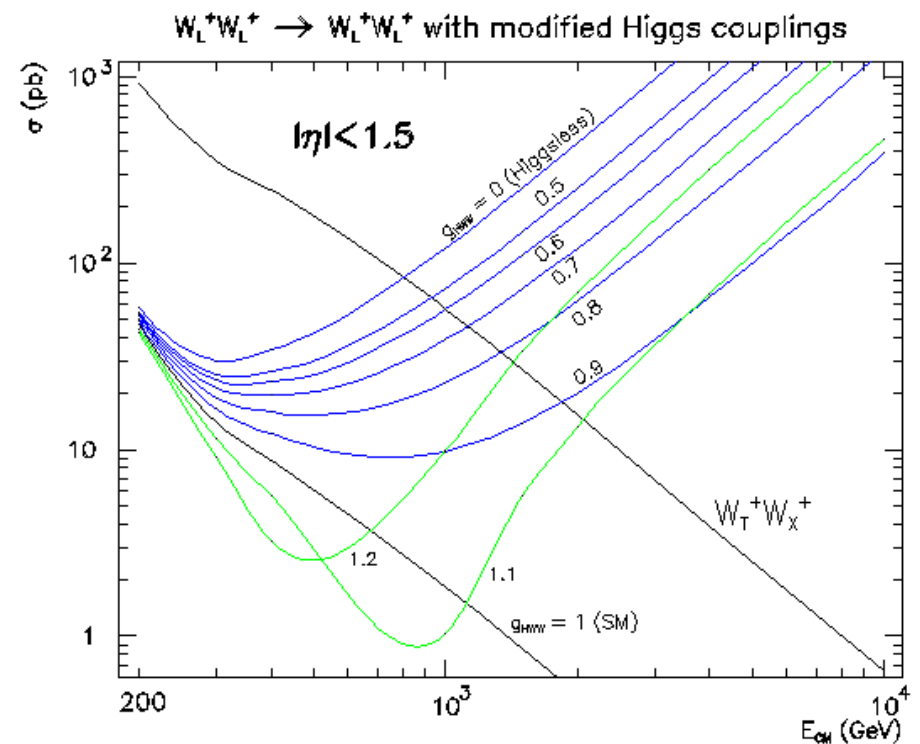
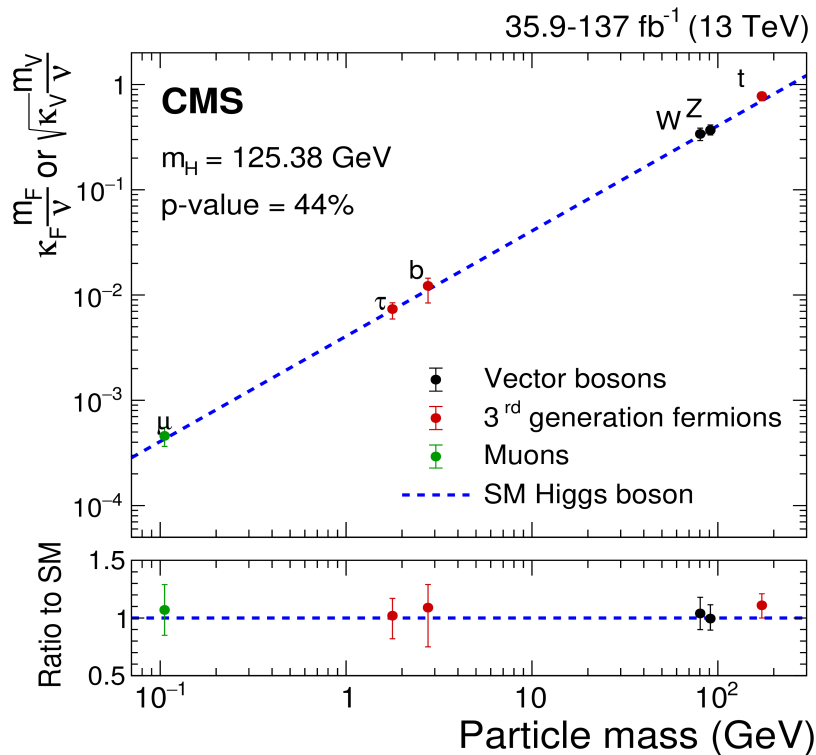
$$\mathcal{M}_H = \frac{g^2}{4M_W^2} s + \mathcal{O}(s^0)$$

- Requirement of unitarity (no divergences) provides an independent, alternative way to derive the Standard Model electroweak sector with the Higgs boson as its key component.
- Do these cancelations really occur? Test of the electroweak symmetry breaking mechanism in the high energy regime - simultaneous probing of 4 couplings.



Vector Boson Scattering as an indirect probe of physics beyond the Standard Model

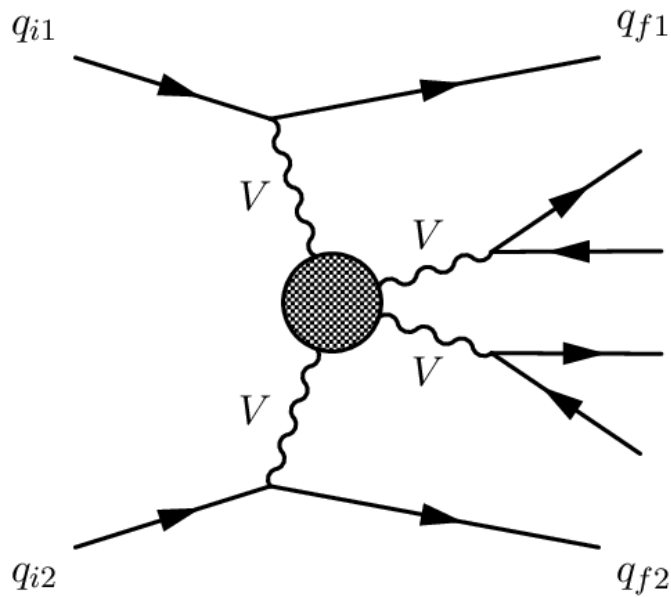
- Only Higgs and gauge couplings equal *exactly* to their Standard Model (SM) values guarantee full cancelation of all divergences without invoking additional particles.
- Standard Model extensions usually predict modified Higgs couplings, e.g., the composite Higgs models – scaled down versions of the Higgsless case



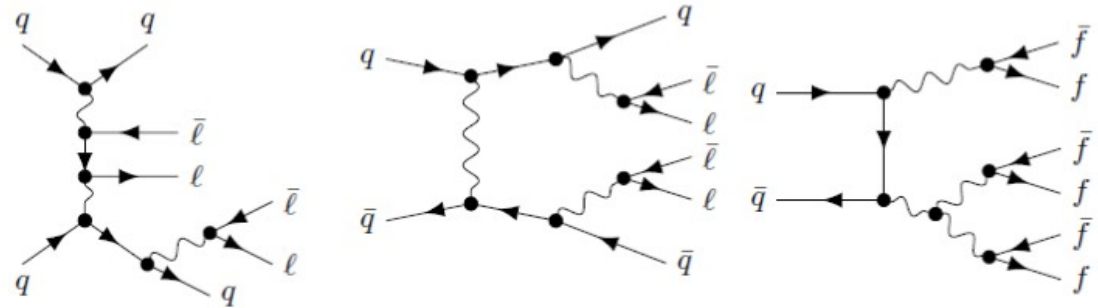
as well as modified effective gauge couplings, e.g.,

- new heavy fermions in loops = anomalous triple coupling (aTGC),
- new heavy particle exchange in the 4W contact graph = anomalous quartic coupling (aQGC)

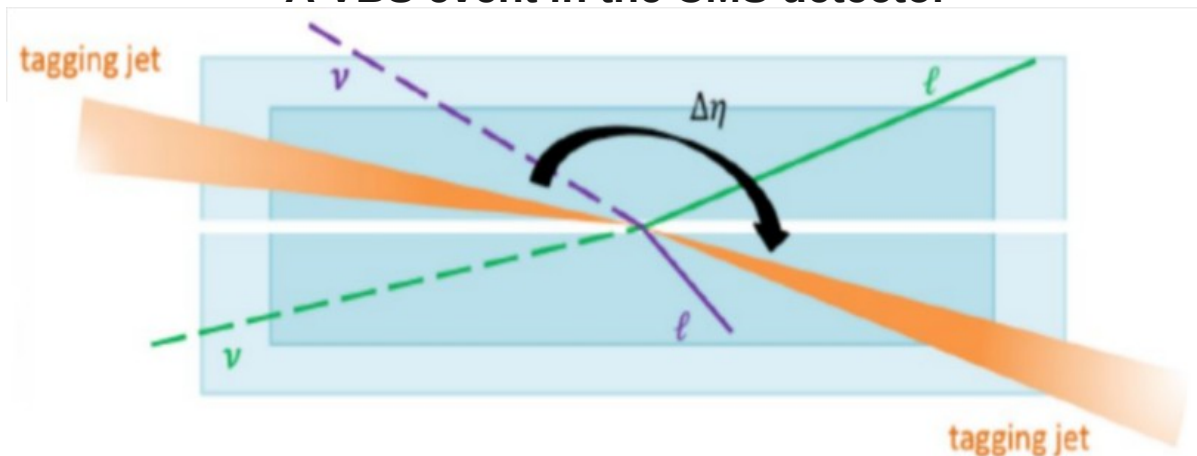
Vector Boson Scattering in a proton-proton collider



- **Signal:** 6 fermions in final state, $\sim \alpha^6$ at leading order
- Signal definition includes non-VBS diagrams which cannot be separated due to gauge invariance

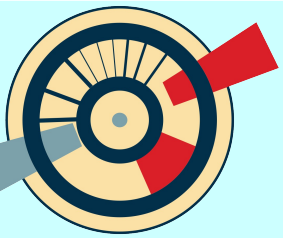


A VBS event in the CMS detector

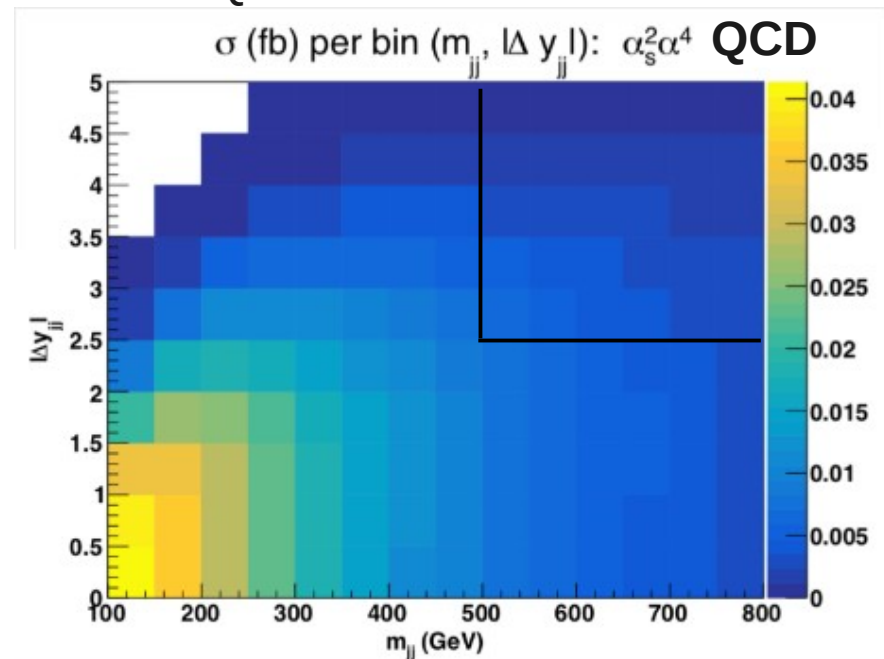
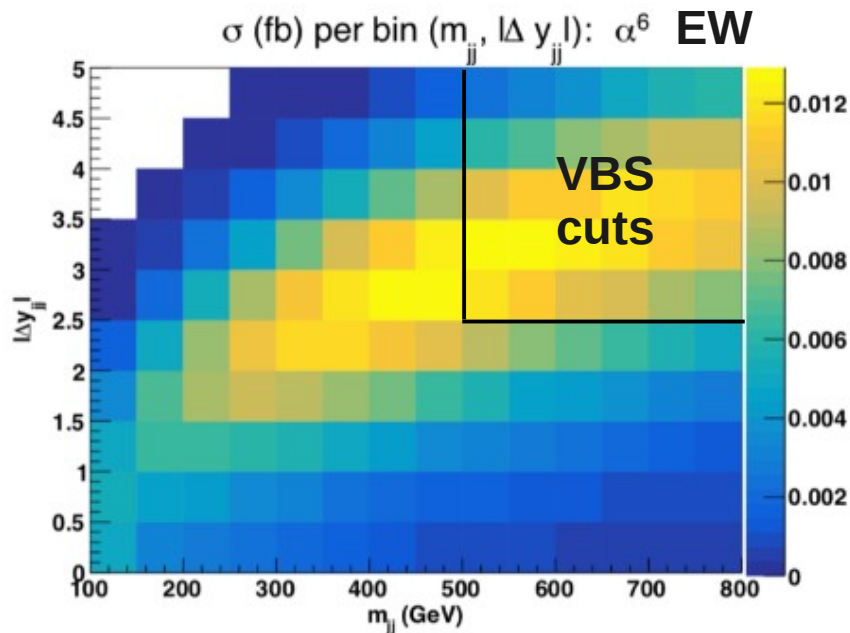
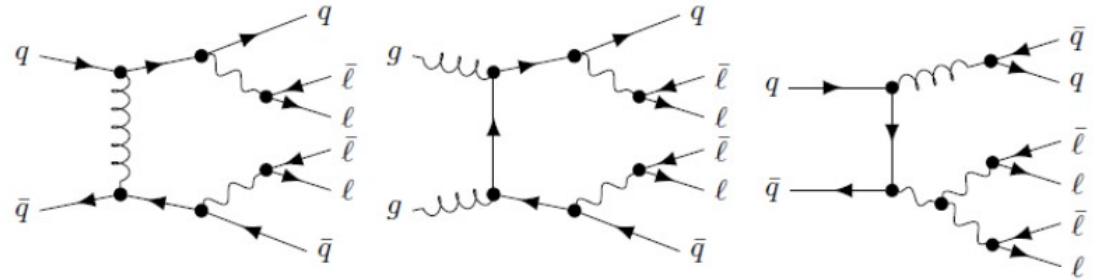


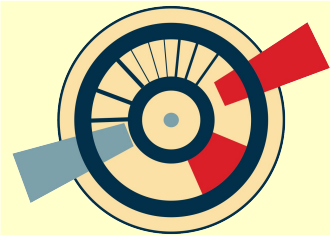
- Two energetic jets with large invariant mass and pseudorapidity separation
- 2, 3 or 4 (depending on process) energetic leptons in the central region

Vector Boson Scattering in a proton-proton collider II



- **Irreducible background:** QCD induced processes leading to the same final state, $\sim \alpha^4 \alpha_s^2$
- **Interference** between EW and QCD, $\sim \alpha^5 \alpha_s$
- **Reducible backgrounds:** various processes with mis-ID of final state particles, usually very detector dependent
- **Other challenges:**
 - Low cross section (typically \sim a few fb)
 - Different polarizations with similar kinematics
 - Reliance on simulation in order to separate EW from QCD





BSM in the language of Effective Quantum Field Theory

Model independent approach to BSM searches:

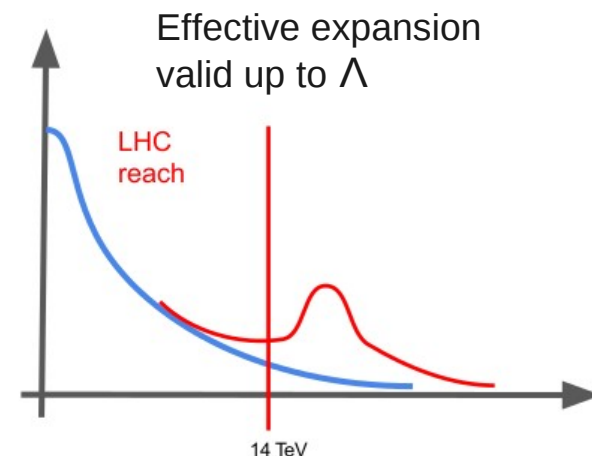
Higher-dimension (dim-6, dim-8, etc.) operators suppressed by appropriate powers of Λ , the energy scale of new physics

$$\mathcal{L}_{EFT} = \mathcal{L}_{SM} + \sum_i \frac{c_i^{(6)}}{\Lambda^2} \mathcal{O}^{(6)} + \frac{c_i^{(8)}}{\Lambda^4} \mathcal{O}^{(8)} + \dots$$

$$f_i^{(6)} = \frac{C_i^{(6)}}{\Lambda^2}, \quad f_i^{(8)} = \frac{C_i^{(8)}}{\Lambda^4}, \dots \quad \text{Wilson Coefficients}$$

dim-6 – affect Higgs couplings, triple gauge couplings and quartic gauge couplings

dim-8 – lowest order operators affecting only quartic gauge couplings

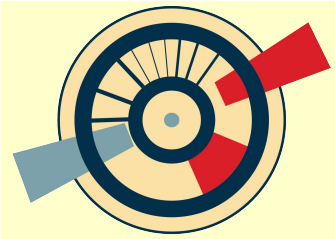


Dim-6 operators relevant to VBS in the Warsaw basis:

- $\mathcal{O}_H = (\Phi^\dagger \Phi)^3$,
- $\mathcal{O}_{HD} = (\Phi^\dagger D_\mu \Phi)^* (\Phi^\dagger D^\mu \Phi)$,
- $\mathcal{O}_{H\Box} = (\Phi^\dagger \Phi) \Box (\Phi^\dagger \Phi)$,

- $\mathcal{O}_W = \epsilon^{ijk} W_\mu^{iv} W_\nu^{j\rho} W_\rho^{k\mu}$,
- $\mathcal{O}_{HW} = H^\dagger H W_{\mu\nu}^I W^{\mu\nu I}$,
- $\mathcal{O}_{HWB} = H^\dagger \tau^I H W_{\mu\nu}^I B^{\mu\nu}$.

Typically studied in Higgs and diboson production processes, VBS not really competitive (or is it?)



Dim-8 operators in VBS

Eboli, Gonzalez-Garcia, arXiv:1604.03555

S (scalar) operators,
affect longitudinal polarizations

$$\mathcal{O}_{S,0} = \left[(D_\mu \Phi)^\dagger D_\nu \Phi \right] \times \left[(D^\mu \Phi)^\dagger D^\nu \Phi \right]$$

$$\mathcal{O}_{S,1} = \left[(D_\mu \Phi)^\dagger D^\mu \Phi \right] \times \left[(D_\nu \Phi)^\dagger D^\nu \Phi \right]$$

T operators, affect
transverse polarizations

$$\mathcal{O}_{T,0} = \text{Tr} \left[\widehat{W}_{\mu\nu} \widehat{W}^{\mu\nu} \right] \times \text{Tr} \left[\widehat{W}_{\alpha\beta} \widehat{W}^{\alpha\beta} \right]$$

$$\mathcal{O}_{T,1} = \text{Tr} \left[\widehat{W}_{\alpha\nu} \widehat{W}^{\mu\beta} \right] \times \text{Tr} \left[\widehat{W}_{\mu\beta} \widehat{W}^{\alpha\nu} \right]$$

$$\mathcal{O}_{T,2} = \text{Tr} \left[\widehat{W}_{\alpha\mu} \widehat{W}^{\mu\beta} \right] \times \text{Tr} \left[\widehat{W}_{\beta\nu} \widehat{W}^{\nu\alpha} \right]$$

$$\mathcal{O}_{T,5} = \text{Tr} \left[\widehat{W}_{\mu\nu} \widehat{W}^{\mu\nu} \right] \times \widehat{B}_{\alpha\beta} \widehat{B}^{\alpha\beta}$$

$$\mathcal{O}_{T,6} = \text{Tr} \left[\widehat{W}_{\alpha\nu} \widehat{W}^{\mu\beta} \right] \times \widehat{B}_{\mu\beta} \widehat{B}^{\alpha\nu}$$

$$\mathcal{O}_{T,7} = \text{Tr} \left[\widehat{W}_{\alpha\mu} \widehat{W}^{\mu\beta} \right] \times \widehat{B}_{\beta\nu} \widehat{B}^{\nu\alpha}$$

$$\mathcal{O}_{T,8} = \widehat{B}_{\mu\nu} \widehat{B}^{\mu\nu} \widehat{B}_{\alpha\beta} \widehat{B}^{\alpha\beta}$$

$$\mathcal{O}_{T,9} = \widehat{B}_{\alpha\mu} \widehat{B}^{\mu\beta} \widehat{B}_{\beta\nu} \widehat{B}^{\nu\alpha}$$

M operators, affect mixed polarizations

$$\mathcal{O}_{M,0} = \text{Tr} \left[\widehat{W}_{\mu\nu} \widehat{W}^{\mu\nu} \right] \times \left[(D_\beta \Phi)^\dagger D^\beta \Phi \right]$$

$$\mathcal{O}_{M,1} = \text{Tr} \left[\widehat{W}_{\mu\nu} \widehat{W}^{\nu\beta} \right] \times \left[(D_\beta \Phi)^\dagger D^\mu \Phi \right]$$

$$\mathcal{O}_{M,2} = \left[\widehat{B}_{\mu\nu} \widehat{B}^{\mu\nu} \right] \times \left[(D_\beta \Phi)^\dagger D^\beta \Phi \right]$$

$$\mathcal{O}_{M,3} = \left[\widehat{B}_{\mu\nu} \widehat{B}^{\nu\beta} \right] \times \left[(D_\beta \Phi)^\dagger D^\mu \Phi \right]$$

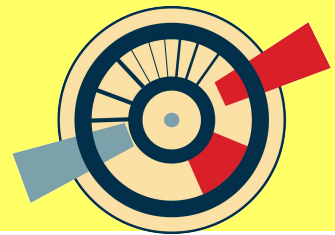
$$\mathcal{O}_{M,4} = \left[(D_\mu \Phi)^\dagger \widehat{W}_{\beta\nu} D^\mu \Phi \right] \times \widehat{B}^{\beta\nu}$$

$$\mathcal{O}_{M,5} = \left[(D_\mu \Phi)^\dagger \widehat{W}_{\beta\nu} D^\nu \Phi \right] \times \widehat{B}^{\beta\mu}$$

$$\mathcal{O}_{M,7} = \left[(D_\mu \Phi)^\dagger \widehat{W}_{\beta\nu} \widehat{W}^{\beta\mu} D^\nu \Phi \right]$$

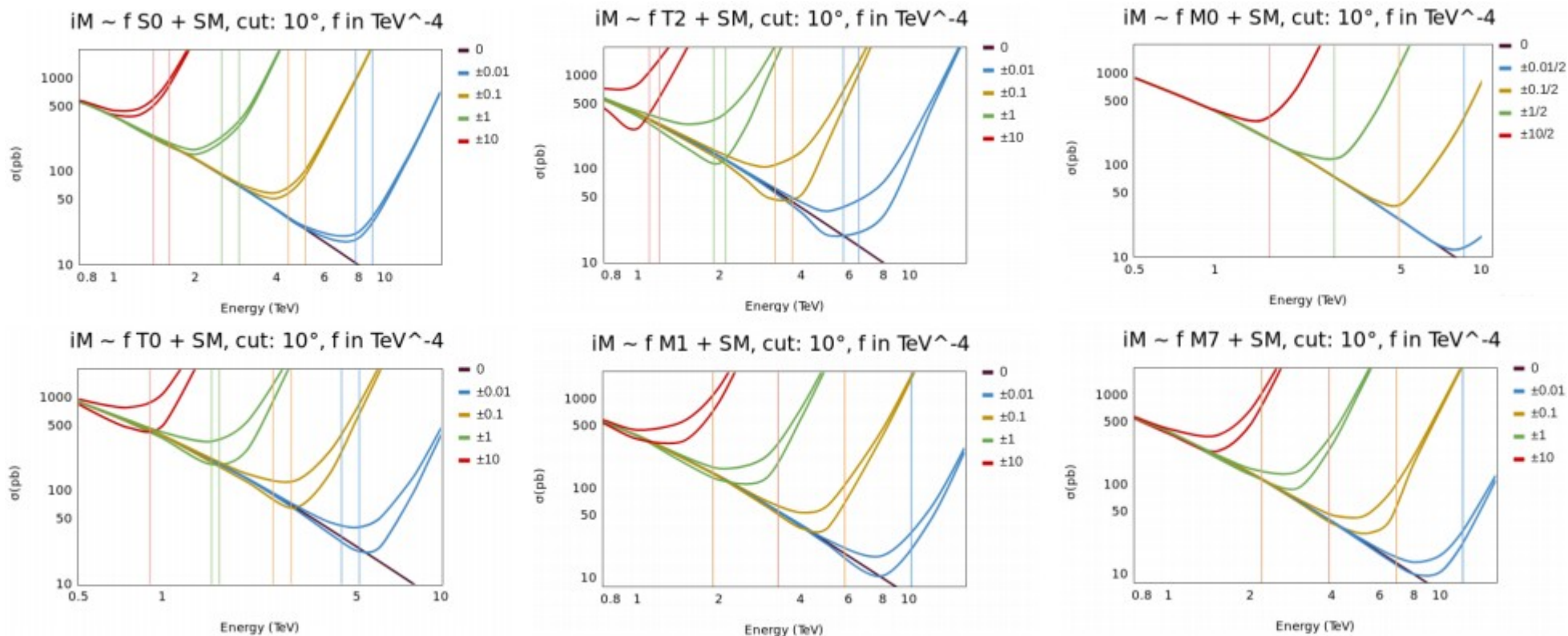
Contribution to the different vertices:

	$\mathcal{O}_{S,0}$	$\mathcal{O}_{M,0}$	$\mathcal{O}_{M,2}$	$\mathcal{O}_{T,0}$	$\mathcal{O}_{T,5}$	$\mathcal{O}_{T,8}$
	$\mathcal{O}_{S,1}$	$\mathcal{O}_{M,1}$	$\mathcal{O}_{M,3}$	$\mathcal{O}_{T,1}$	$\mathcal{O}_{T,6}$	$\mathcal{O}_{T,9}$
	$\mathcal{O}_{S,2}$	$\mathcal{O}_{M,7}$	$\mathcal{O}_{M,4}$	$\mathcal{O}_{T,2}$	$\mathcal{O}_{T,7}$	$\mathcal{O}_{T,9}$
	$\mathcal{O}_{M,5}$					
WWWW	X	X		X		
WWZZ	X	X	X	X	X	
ZZZZ	X	X	X	X	X	X
WWZ γ		X	X	X	X	
WW $\gamma\gamma$		X	X	X	X	
ZZZ γ		X	X	X	X	X
ZZ $\gamma\gamma$		X	X	X	X	X
Z $\gamma\gamma\gamma$				X	X	X
$\gamma\gamma\gamma\gamma$				X	X	X

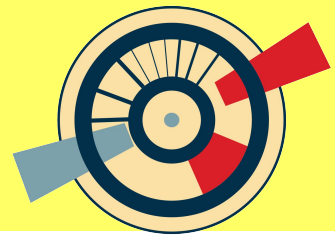


VV cross section with aQGC

Total $W^+W^+ \rightarrow W^+W^+$ cross section (on shell) for different dim-8 operators: S0, T2, M0, T0, M1 and M7



Measureable BSM effects are confined to a narrow energy range just before the unitarity limit (vertical lines)



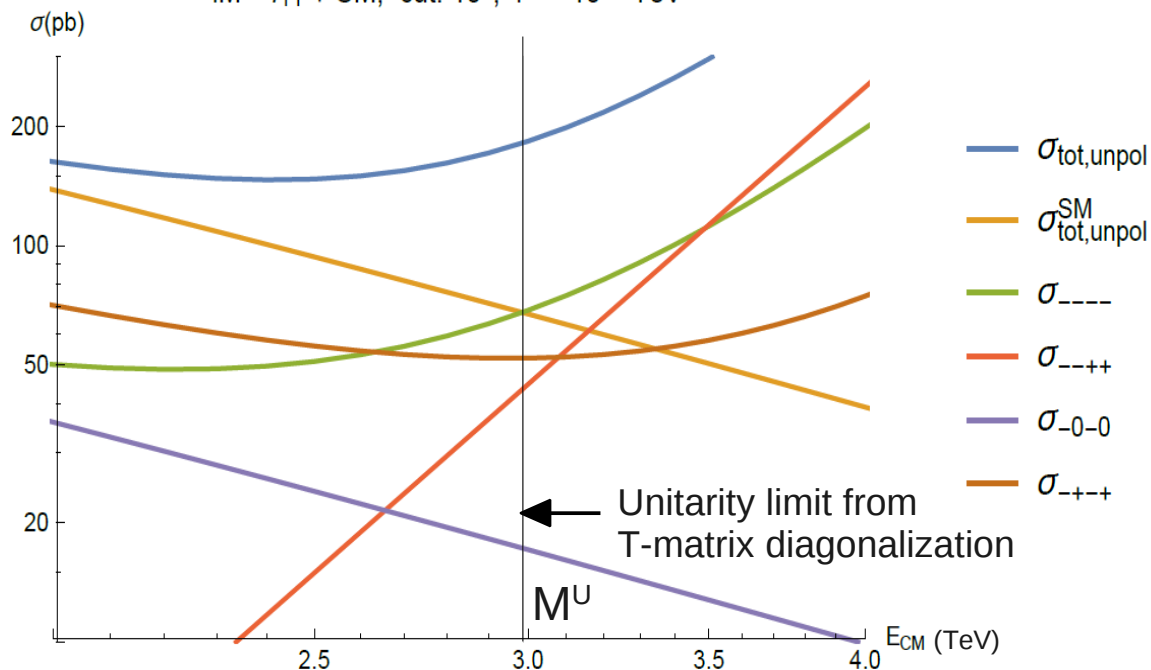
Helicities and unitarity limits

W^+W^+ scattering process - 13 independent helicity combinations

Example: the case of non-zero f_{T1}

Unitarity limits M^U (in TeV)
for individual amplitudes

$iM \sim f_{T1} + SM$, cut: 10° , $f = -10^{-1} \text{ TeV}^{-4}$



Hel. \ $f_{T1} =$	-0.01	-0.1	-1.	-10.
----0	5.3	3.0	1.7	0.96
----+	7.5×10^7	7.5×10^6	7.5×10^5	7.5×10^4
--00	1.7×10^3	530.	170.	53.
--0+	440.	140.	44.	14.
--++	74.	34.	16.	7.4
--00	5.5	3.1	1.7	0.99
-0-0	2.5×10^3	800.	250.	80.
-0-+	69.	32.	15.	6.9
-000	3.7×10^7	3.7×10^6	3.7×10^5	3.7×10^4
-00+	2.3×10^3	740.	230.	74.
-+++	10.	5.6	3.2	1.8
-+00	1.7×10^3	530.	170.	53.
0000	x	x	x	x

Total $W^+W^+ \rightarrow W^+W^+$ cross section for $f_{T1} = -0.1/\text{TeV}^4$
split into initial & final state helicity combinations

The unitarity problem and how we deal with it

- It is well known that every dim-8 operator causes amplitude growth which behaves asymptotically as $\sim s^2$ and eventually leads to unitarity violation.
- In the range of Wilson coefficients experiments at the LHC are currently sensitive to, unitarity violation occurs well within the measured kinematic range.

Philosophy 1. Disregard unitarity limits (CMS mainstream)

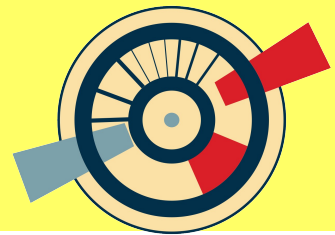
- technical simplicity,
- only to quantify the relative precision of different measurements and the degree of agreement/disagreement with the SM,
- **obtained numbers do not have direct EFT interpretation.**

Philosophy 2. Unitarization techniques:

Saturation of amplitude: K-matrix method (ATLAS mainstream)

- describe the maximum possible signal related to a given operator,
- other popular approaches to unitarization: the Inverse Amplitude Method, N/D method, Form factor method (e.g. VBFNLO), explicit resonances (e.g. WHIZARD),
- different results, **breaks model independence of the EFT approach.**
- more in: Alboteanu et al. arXiv:0806.4145, Kilian et al. arXiv:1408.6207, Perez et al. arXiv:1807.02707.

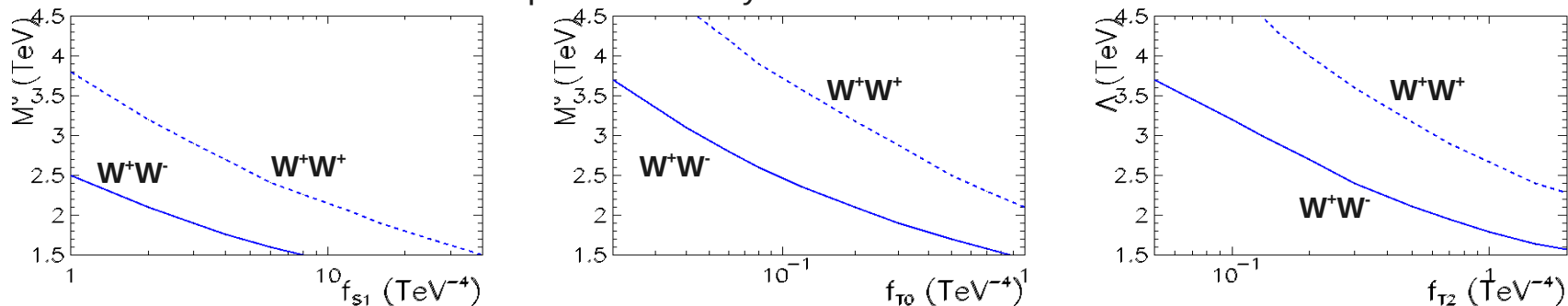
- Side remark: **We should never directly compare ATLAS numbers with CMS numbers!**



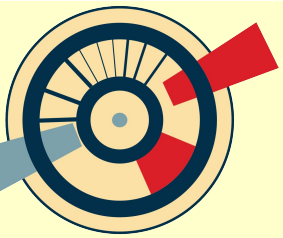
Unitarity and the EFT validity cutoff

1. EFT validity stops at $M_{VV}=\Lambda$, the scale of new physics. Λ can be *maximally* equal to the relevant unitarity limit, but it may as well be *lower* than that, $\Lambda \leq M^U$. The actual value of Λ is *unknown a priori* and can only be deduced from the data.
2. For a given operator Λ is one value, it applies to all affected amplitudes, even though their individual unitarity limits can be much higher. Relevant e.g. to helicity combinations.
3. Λ must be common to different processes if they probe the same coupling (same set of higher dimension operators). For instance, the W^+W^- scattering process reaches unitarity limit *before* W^+W^+ for most dim-8 operators: O_{S1} , O_{T0} , O_{T1} (positive f), O_{T2} , O_{M0} , O_{M1} and O_{M7} .

Examples of unitarity limits for W^+W^+ and W^+W^-

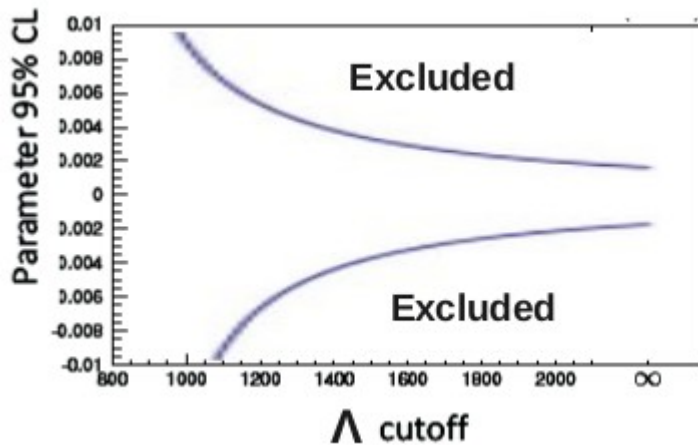
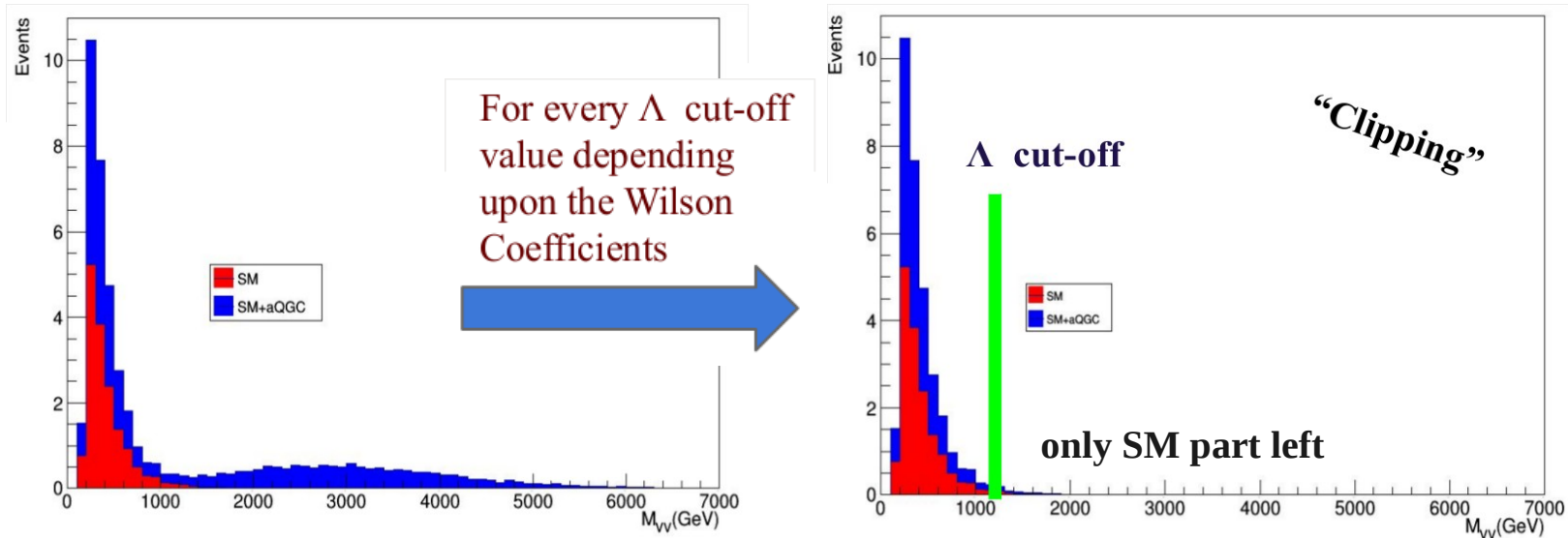


The same goes for $WZ \rightarrow WZ$ and $WW \rightarrow ZZ$: same $WWZZ$ coupling, ZZ usually breaks unitarity faster.



How to set limits on BSM in the EFT framework: “clipping method”

- The EFT does not predict what happens above Λ . Only the most conservative limits are guaranteed to be true. Most conservative = cut at Λ or assume SM.



Data outside of the EFT validity region are not used (ZZ) or assumed to be SM-like if direct omission is not possible (WW and WZ, we do not measure the VV invariant mass)

- Limits on Wilson coefficients can only be determined as a function of Λ – 2-dimensional exclusion curves.

VBS analyses published up to date by CMS

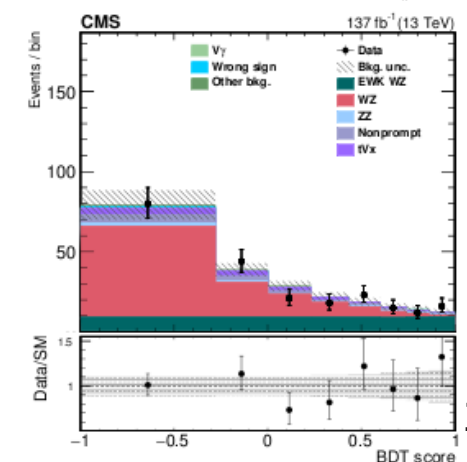
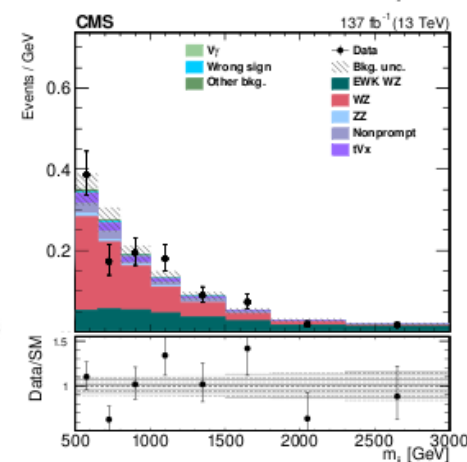
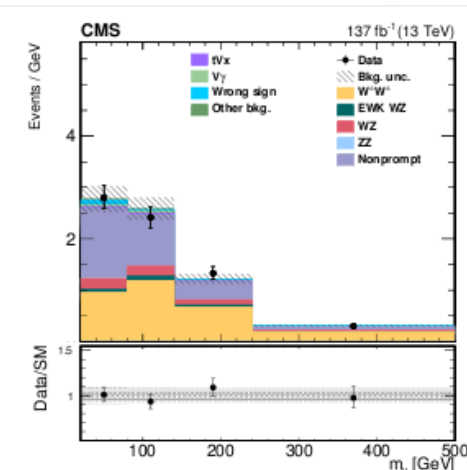
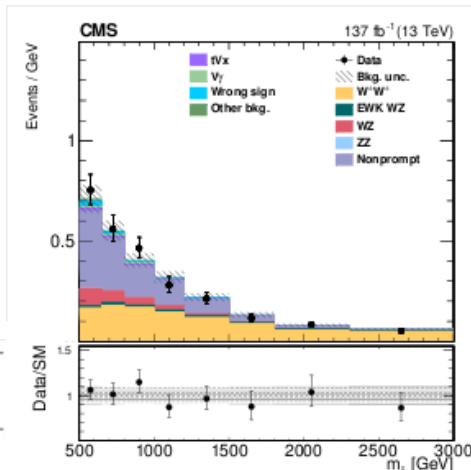
CADI	Analysis	Journal
SMP-20-016	Zγjj	<u>CDS preliminary result</u>
SMP-20-006	Polarized W\pmW\pmjj	<u>PLB 812 (2020) 136018</u>
SMP-20-001	ZZjj	<u>PLB 812 (2020) 135992</u>
SMP-19-008	Wγjj (2016 data)	<u>PLB 811 (2020) 135988</u>
SMP-19-012	W\pmW\pmjj and WZjj	<u>PLB 809 (2020) 135710</u>
SMP-18-007	Z γ jj (2016 data)	<u>JHEP 06 (2020) 076</u>
SMP-18-006	VVjj (2016 data)	<u>PLB 798 (2019)134985</u>
SMP-18-001	WZjj (2016 data)	<u>PLB 795 (2019) 281</u>
SMP-17-004	W \pm W \pm jj (2016 data)	<u>PRL 120 081801 (2018)</u>
SMP-17-006	ZZjj (2016 data)	<u>PLB 774 (2017) 682</u>
SMP-16-018	Zjj (2016 data)	<u>EPJC 78 (2018) 589</u>

CMS: Same-sign WWjj and WZjj electroweak production

SMP-19-012, arXiv:2005.01173

- Whole Run 2 (137/fb)
- Fully leptonic final states
- Signal significance: $\gg 5$ sigma for ssWW (was 5 sigma from 2016 data alone), 6.8 obs. (5.3 exp.) for WZ
- Inclusive and differential cross sections consistent with SM predictions

Variable	$W^\pm W^\pm$	WZ
Leptons	2 leptons, $p_T > 25/20$ GeV	3 leptons, $p_T > 25/10/20$ GeV
p_T^j	> 50 GeV	> 50 GeV
$ m_{\ell\ell} - m_Z $	> 15 GeV (ee)	< 15 GeV
$m_{\ell\ell}$	> 20 GeV	—
$m_{\ell\ell\ell}$	—	> 100 GeV
p_T^{miss}	> 30 GeV	> 30 GeV
b quark veto	Required	Required
$\max(z_\ell^*)$	< 0.75	< 1.0
m_{jj}	> 500 GeV	> 500 GeV
$ \Delta\eta_{jj} $	> 2.5	> 2.5



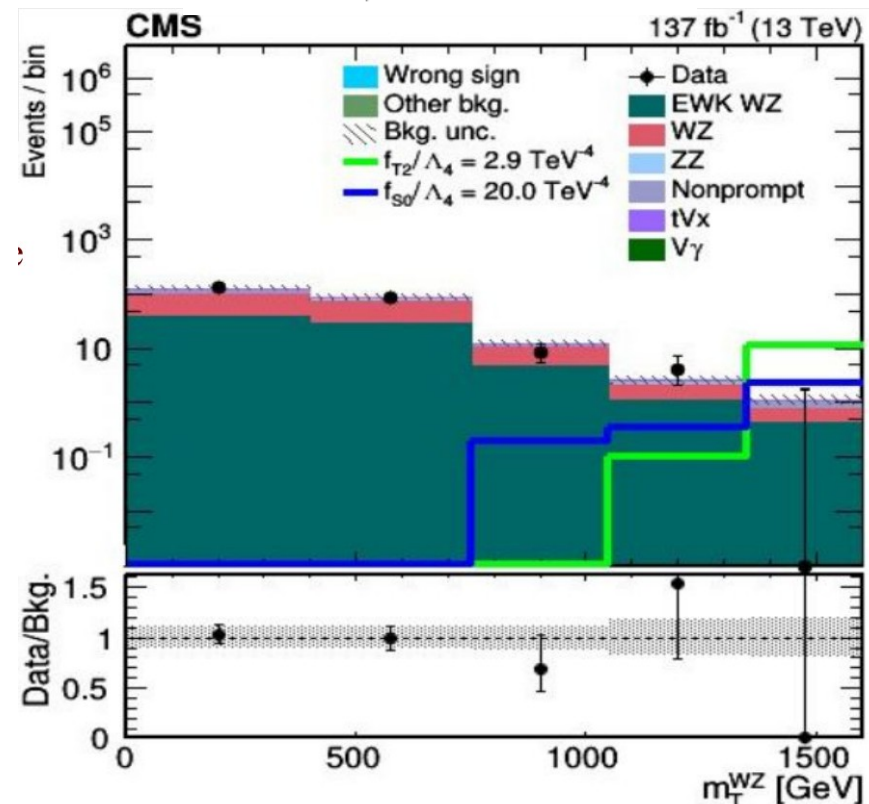
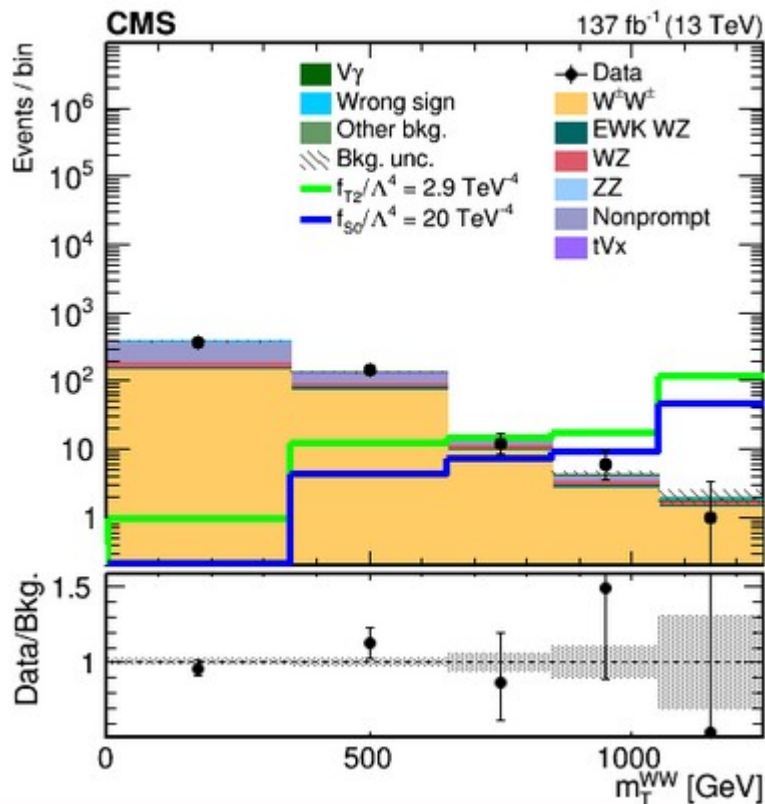
Process	σB (fb)	Theoretical prediction without NLO corrections (fb)	Theoretical prediction with NLO corrections (fb)
EW $W^\pm W^\pm$	3.98 ± 0.45 $0.37(\text{stat}) \pm 0.25(\text{syst})$	3.93 ± 0.57	3.31 ± 0.47
EW+QCD $W^\pm W^\pm$	4.42 ± 0.47 $0.39(\text{stat}) \pm 0.25(\text{syst})$	4.34 ± 0.69	3.72 ± 0.59
EW WZ	1.81 ± 0.41 $0.39(\text{stat}) \pm 0.14(\text{syst})$	1.41 ± 0.21	1.24 ± 0.18
EW+QCD WZ	4.97 ± 0.46 $0.40(\text{stat}) \pm 0.23(\text{syst})$	4.54 ± 0.90	4.36 ± 0.88
QCD WZ	3.15 ± 0.49 $0.45(\text{stat}) \pm 0.18(\text{syst})$	3.12 ± 0.70	3.12 ± 0.70

“Clipping” technique in implementation

- **First implementation of a partial “clipping” technique in CMS**

- Simulated distribution "clipped" at the unitarity limit depending on the Wilson coefficient,
- Typical unitarity limits for dim-8 operators in the relevant range: ~ 1.5 TeV,
- Typical fraction of generated events (aQGC samples) above unitarity limit: up to $\sim 50\%$ for WZ and up to $\sim 80\%$ for ssWW

$$m_T(VV) = \sqrt{\left(\sum_i E_i\right)^2 - \left(\sum_i p_{z,i}\right)^2}$$



Results – current limits on BSM physics

Conventional procedure (unitarity condition disregarded)

	Observed ($W^\pm W^\pm$) (TeV^{-4})	Expected ($W^\pm W^\pm$) (TeV^{-4})	Observed (WZ) (TeV^{-4})	Expected (WZ) (TeV^{-4})	Observed (TeV^{-4})	Expected (TeV^{-4})
f_{T0}/Λ^4	[-0.28, 0.31]	[-0.36, 0.39]	[-0.62, 0.65]	[-0.82, 0.85]	[-0.25, 0.28]	[-0.35, 0.37]
f_{T1}/Λ^4	[-0.12, 0.15]	[-0.16, 0.19]	[-0.37, 0.41]	[-0.49, 0.55]	[-0.12, 0.14]	[-0.16, 0.19]
f_{T2}/Λ^4	[-0.38, 0.50]	[-0.50, 0.63]	[-1.0, 1.3]	[-1.4, 1.7]	[-0.35, 0.48]	[-0.49, 0.63]
f_{M0}/Λ^4	[-3.0, 3.2]	[-3.7, 3.8]	[-5.8, 5.8]	[-7.6, 7.6]	[-2.7, 2.9]	[-3.6, 3.7]
f_{M1}/Λ^4	[-4.7, 4.7]	[-5.4, 5.8]	[-8.2, 8.3]	[-11, 11]	[-4.1, 4.2]	[-5.2, 5.5]
f_{M6}/Λ^4	[-6.0, 6.5]	[-7.5, 7.6]	[-12, 12]	[-15, 15]	[-5.4, 5.8]	[-7.2, 7.3]
f_{M7}/Λ^4	[-6.7, 7.0]	[-8.3, 8.1]	[-10, 10]	[-14, 14]	[-5.7, 6.0]	[-7.8, 7.6]
f_{S0}/Λ^4	[-6.0, 6.4]	[-6.0, 6.2]	[-19, 19]	[-24, 24]	[-5.7, 6.1]	[-5.9, 6.2]
f_{S1}/Λ^4	[-18, 19]	[-18, 19]	[-30, 30]	[-38, 39]	[-16, 17]	[-18, 18]

“Partial clipping” - unitarity observed

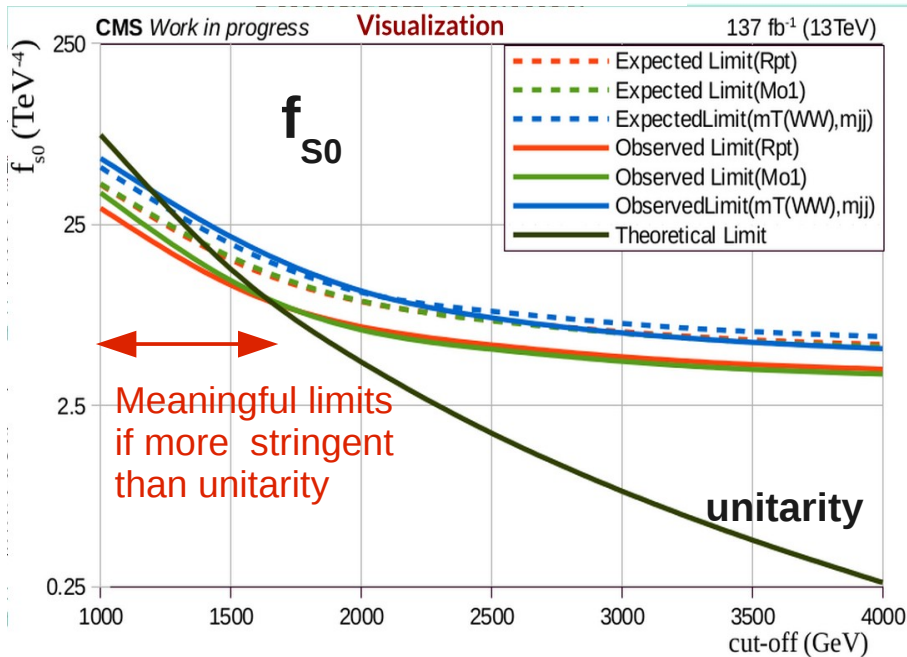
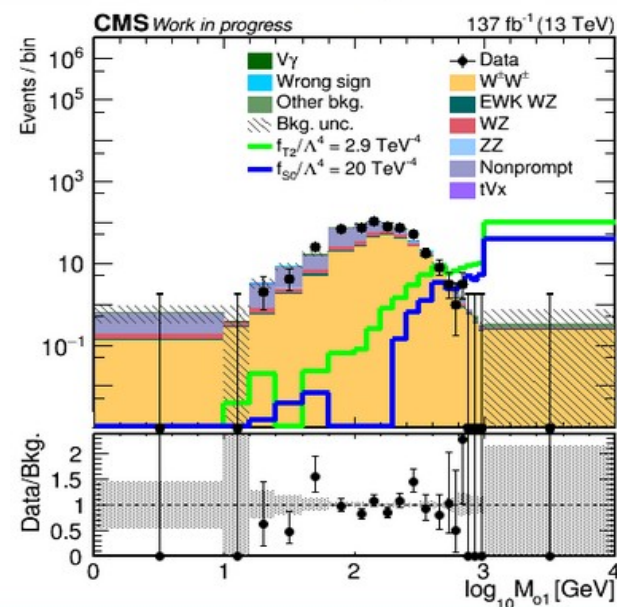
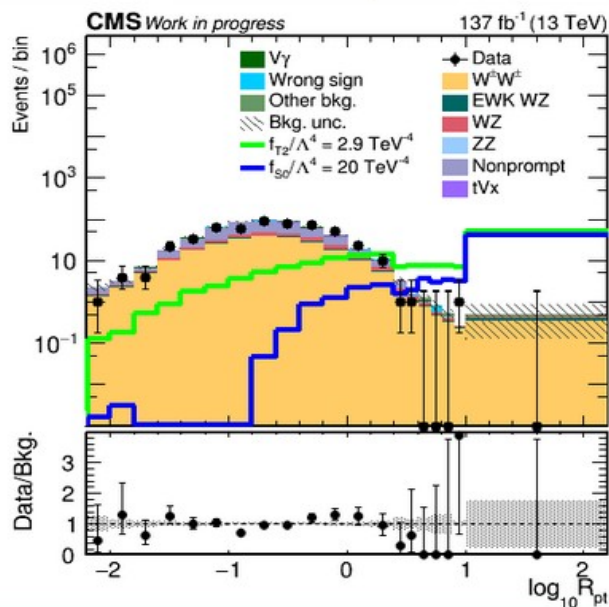
	Observed ($W^\pm W^\pm$) (TeV^{-4})	Expected ($W^\pm W^\pm$) (TeV^{-4})	Observed (WZ) (TeV^{-4})	Expected (WZ) (TeV^{-4})	Observed (TeV^{-4})	Expected (TeV^{-4})
f_{T0}/Λ^4	[-1.5, 2.3]	[-2.1, 2.7]	[-1.6, 1.9]	[-2.0, 2.2]	[-1.1, 1.6]	[-1.6, 2.0]
f_{T1}/Λ^4	[-0.81, 1.2]	[-0.98, 1.4]	[-1.3, 1.5]	[-1.6, 1.8]	[-0.69, 0.97]	[-0.94, 1.3]
f_{T2}/Λ^4	[-2.1, 4.4]	[-2.7, 5.3]	[-2.7, 3.4]	[-4.4, 5.5]	[-1.6, 3.1]	[-2.3, 3.8]
f_{M0}/Λ^4	[-13, 16]	[-19, 18]	[-16, 16]	[-19, 19]	[-11, 12]	[-15, 15]
f_{M1}/Λ^4	[-20, 19]	[-22, 25]	[-19, 20]	[-23, 24]	[-15, 14]	[-18, 20]
f_{M6}/Λ^4	[-27, 32]	[-37, 37]	[-34, 33]	[-39, 39]	[-22, 25]	[-31, 30]
f_{M7}/Λ^4	[-22, 24]	[-27, 25]	[-22, 22]	[-28, 28]	[-16, 18]	[-22, 21]
f_{S0}/Λ^4	[-35, 36]	[-31, 31]	[-83, 85]	[-88, 91]	[-34, 35]	[-31, 31]
f_{S1}/Λ^4	[-100, 120]	[-100, 110]	[-110, 110]	[-120, 130]	[-86, 99]	[-91, 97]

Limits weaker by a factor ~4-5 by only considering unitarity

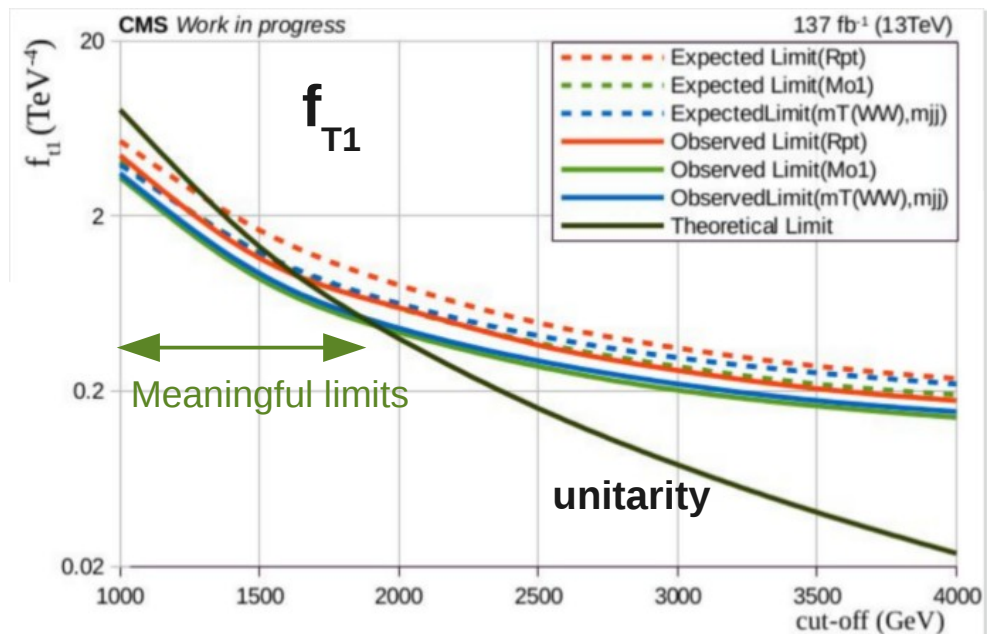
Followup of the ssWW analysis

- Studies of new variables with better sensitivity to BSM effects
- Calculation of limits as a function of the Λ cutoff

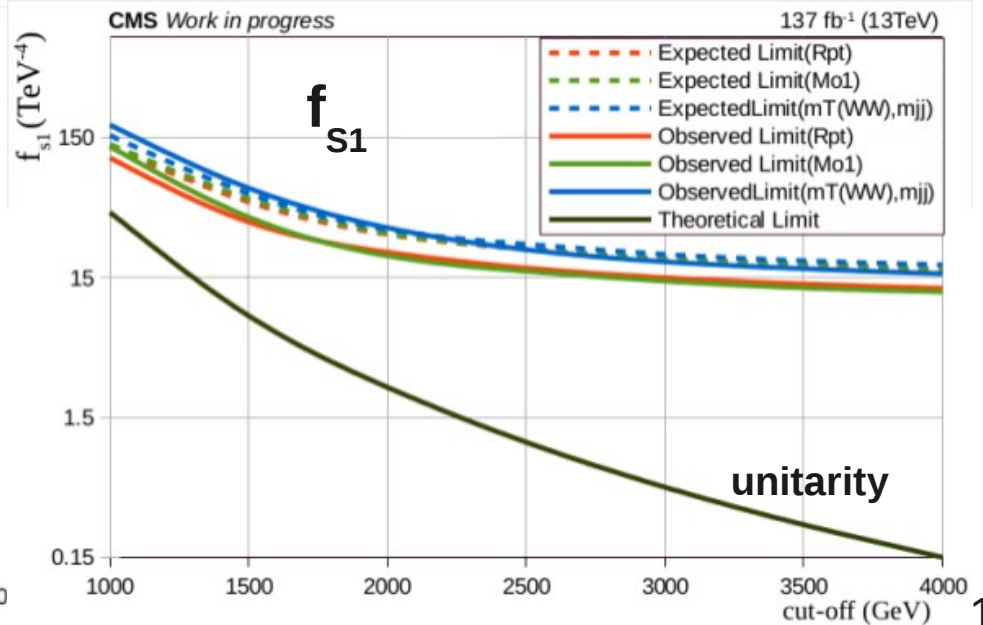
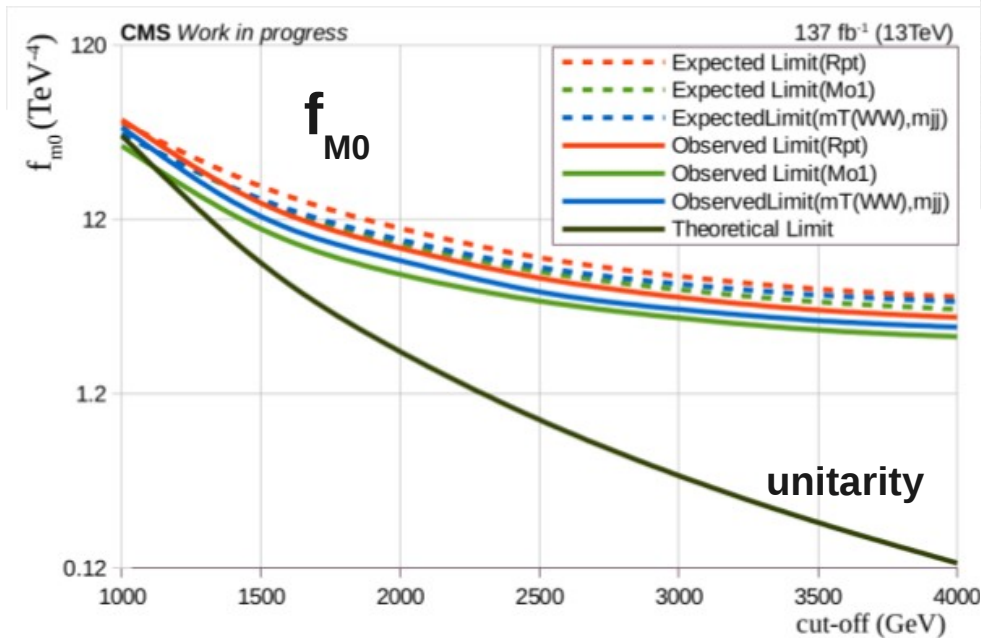
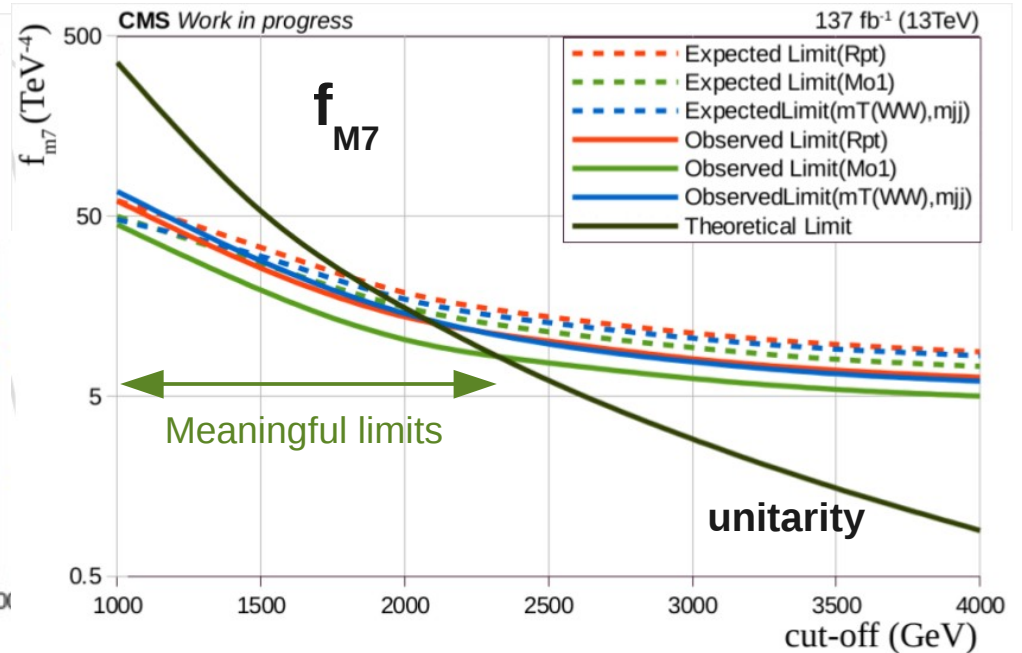
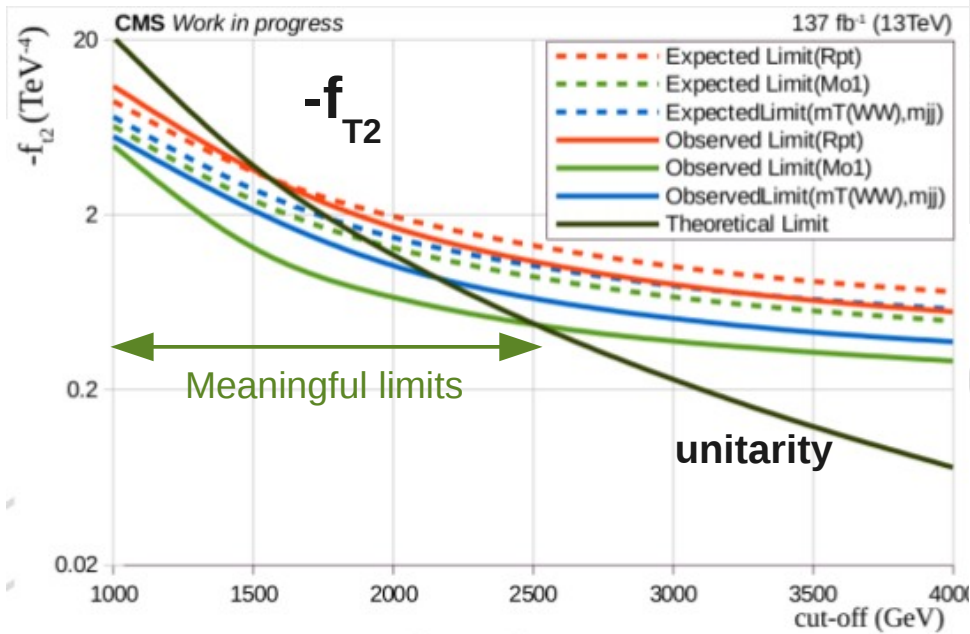
$$R_{pt} = (p_T^{l1} * p_T^{l2}) / (p_T^{j1} * p_T^{j2})$$



$$M_{o1} \equiv \sqrt{(|\vec{p}_T^{l1}| + |\vec{p}_T^{l2}| + |\vec{p}_T^{miss}|)^2 - (\vec{p}_T^{l1} + \vec{p}_T^{l2} + \vec{p}_T^{miss})^2}$$



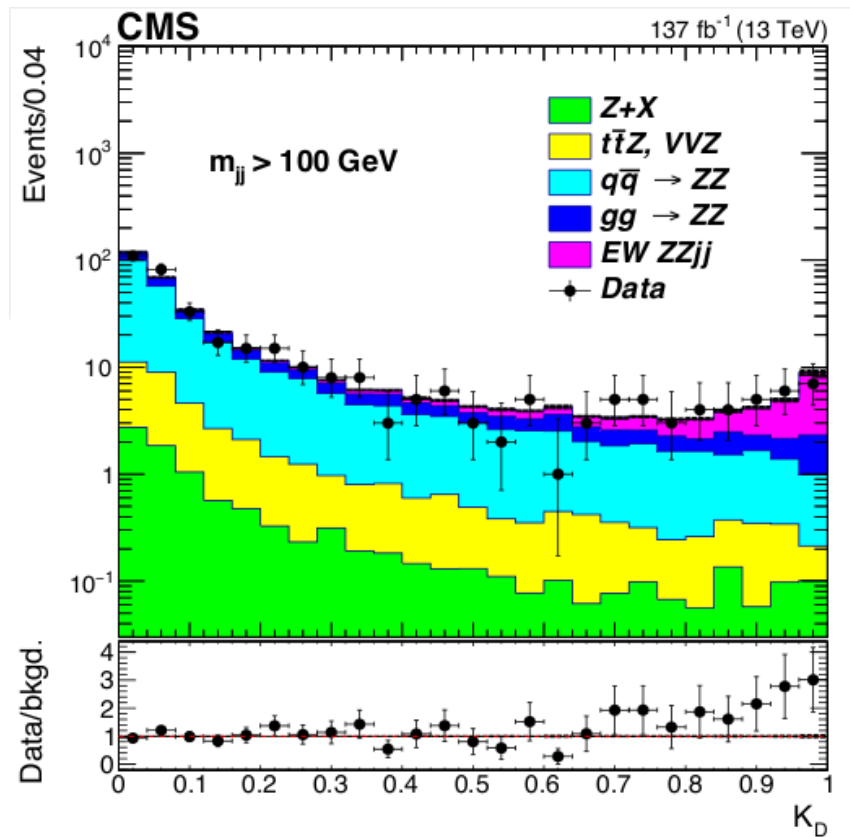
First results of "full clipping" – the best and the worst



CMS: ZZjj electroweak production

- Evidence of electroweak production at 4.0 sigma (expected 3.5) Z and ZZ
- Dominated by QCD irreducible background qq ZZjj and gg ZZjj, a matrix element discriminant used to separate the EW signal
- Fiducial cross section measured in 3 different phase spaces

Particle type	Selection
ZZjj inclusive	
Leptons	$p_T(\ell_1) > 20 \text{ GeV}$ $p_T(\ell_2) > 10 \text{ GeV}$ $p_T(\ell) > 5 \text{ GeV}$ $ \eta(\ell) < 2.5$
Z and ZZ	$60 < m(\ell\ell) < 120 \text{ GeV}$ $m(4\ell) > 180 \text{ GeV}$
Jets	at least 2 $p_T(j) > 30 \text{ GeV}$ $ \eta(j) < 4.7$ $m_{jj} > 100 \text{ GeV}$ $\Delta R(\ell, j) > 0.4$ for each ℓ, j
VBS-enriched (loose)	
Jets	ZZjj inclusive + $ \Delta\eta_{jj} > 2.4$ $m_{jj} > 400 \text{ GeV}$
VBS-enriched (tight)	
Jets	ZZjj inclusive + $ \Delta\eta_{jj} > 2.4$ $m_{jj} > 1 \text{ TeV}$



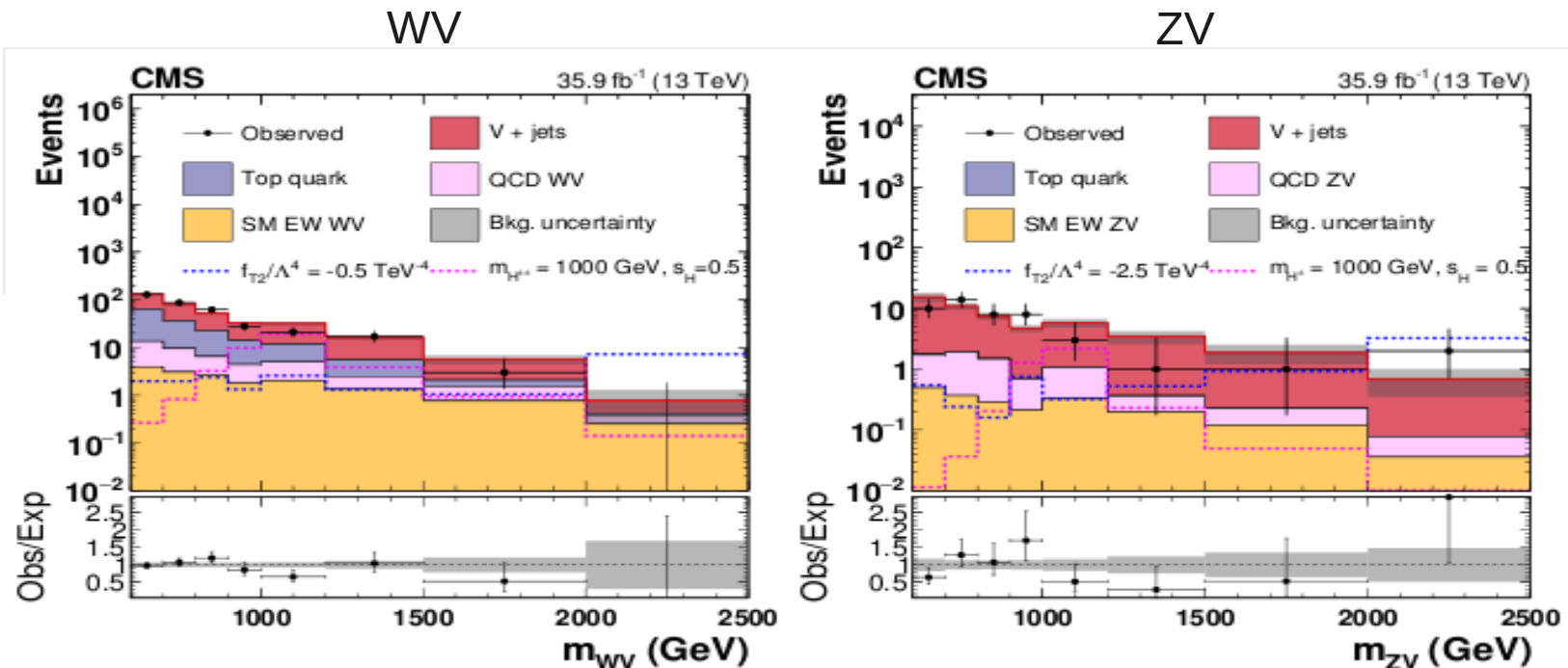
[arXiv:2008.07013](https://arxiv.org/abs/2008.07013)

	Perturbative order	SM σ (fb)	Measured σ (fb)
ZZjj inclusive			
EW	LO	0.275 ± 0.021	
	NLO QCD	0.278 ± 0.017	$0.33^{+0.11}_{-0.10} \text{ (stat)}^{+0.04}_{-0.03} \text{ (syst)}$
	NLO EW	$0.242^{+0.015}_{-0.013}$	
EW+QCD		5.35 ± 0.51	$5.29^{+0.31}_{-0.30} \text{ (stat)} \pm 0.47 \text{ (syst)}$
VBS-enriched (loose)			
EW	LO	0.186 ± 0.015	
	NLO QCD	0.197 ± 0.013	$0.180^{+0.070}_{-0.060} \text{ (stat)}^{+0.021}_{-0.012} \text{ (syst)}$
EW+QCD		1.21 ± 0.09	$1.00^{+0.12}_{-0.11} \text{ (stat)} \pm 0.07 \text{ (syst)}$
VBS-enriched (tight)			
EW	LO	0.104 ± 0.008	
	NLO QCD	0.108 ± 0.007	$0.09^{+0.04}_{-0.03} \text{ (stat)} \pm 0.02 \text{ (syst)}$
EW+QCD		0.221 ± 0.014	$0.20^{+0.05}_{-0.04} \text{ (stat)} \pm 0.02 \text{ (syst)}$

WVjj + ZVjj electroweak production (with one V=W,Z decaying hadronically)

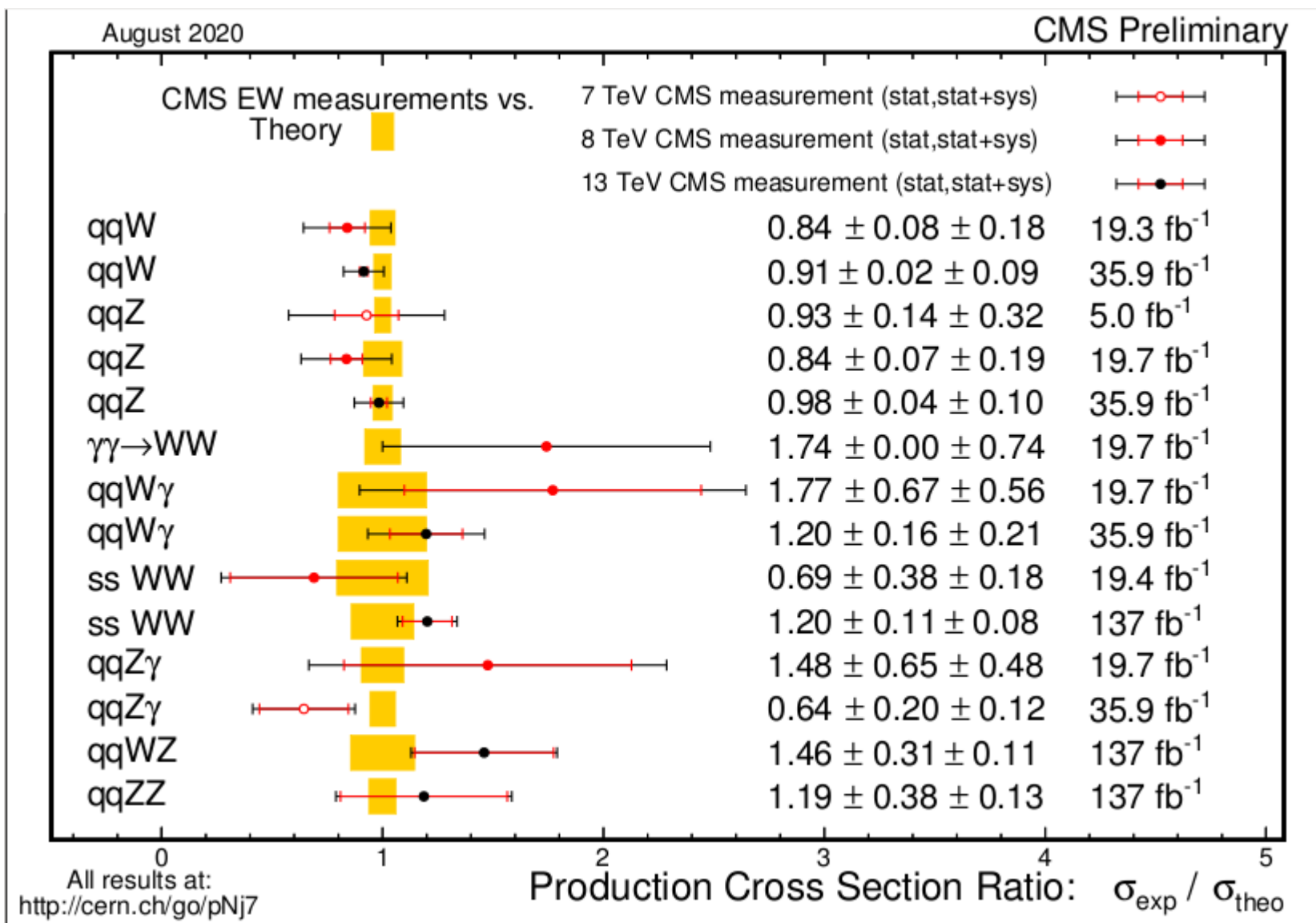
arXiv:1905.07445

- Based on 2016 data only (36/fb).
- Includes ssWW, osWW, WZ and ZZ, much higher statistics, but harder background.
- Hadronic V reconstructed as one large-radius jet.
- Jet substructure techniques used to discriminate 2-prong objects arising from V decays from ordinary light quark and gluon jets. N-subjettiness [*arXiv:1011.2268*] quantifies how well a jet can be divided into N subjets. V-tag efficiency $\sim 70\%$, mistag rate $\sim 5\%$.
- Tight selection criteria to enhance sensitivity to aQGCs.



Other channels – summary of cross section measurements by CMS

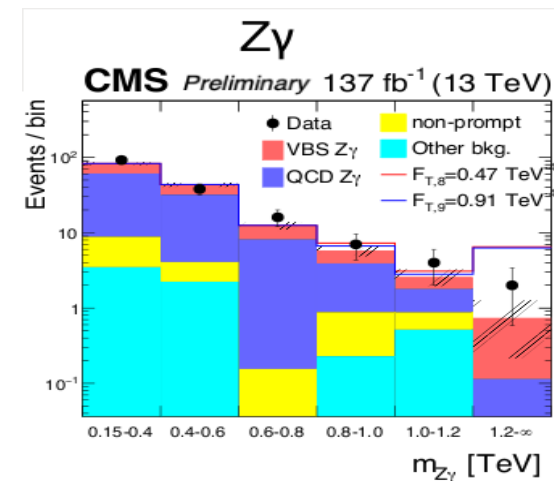
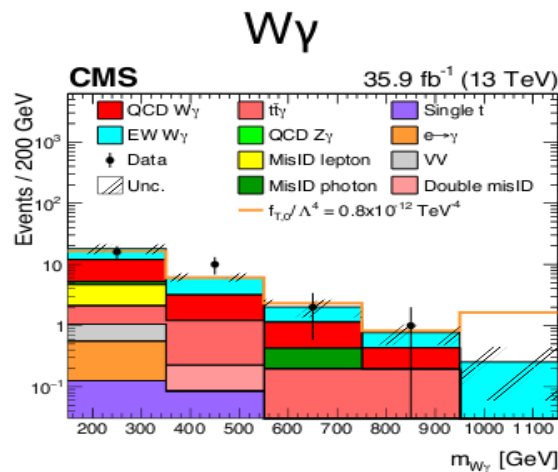
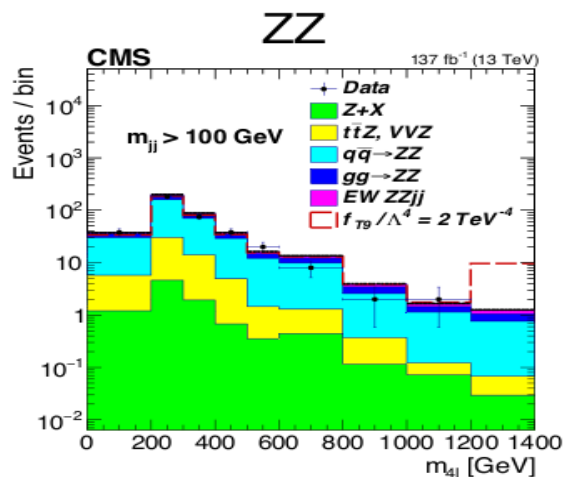
- **Z γ** – preliminary result available (whole Run 2) – 5 sigma observation
- **W γ** – based on 2016 data only (36/fb) – 5 sigma observation



Anomalous Quartic Couplings – CMS summary

	SMP-20-001 <i>ZZ</i>	SMP-19-012 <i>ssWW + WZ</i>	SMP-19-008 <i>Wγ</i>	SMP-20-016 <i>Zγ</i>	SMP-19-006 <i>WV + ZV</i>
f_{T0}	-0.24, 0.22	-0.25, 0.28	-0.60, 0.64	-0.64, 0.57	-0.12, 0.11
f_{T1}	-0.31, 0.31	-0.12, 0.14	-0.35, 0.39	-0.81, 0.90	-0.12, 0.13
f_{T2}	-0.63, 0.59	-0.49, 0.63	-0.99, 1.18	-1.7, 1.5	-0.28, 0.28
f_{T5}			-0.45, 0.46	-0.58, 0.64	
f_{T6}			-0.36, 0.38	-1.3, 1.3	
f_{T7}			-0.87, 0.93	-2.2, 2.4	
f_{T8}	-0.43, 0.43			-0.47, 0.47	
f_{T9}	-0.92, 0.92			-0.91, 0.91	
f_{M0}		-2.7, 2.9	-8.1, 8.0	-16, 16	-0.69, 0.70
f_{M1}		-4.1, 4.2	-12, 12	-35, 35	-2.0, 2.1
f_{M2}			-2.8, 2.8	-6.6, 6.5	
f_{M3}			-4.4, 4.4	-13, 13	
f_{M4}			-5.0, 5.0	-13, 13	
f_{M5}			-8.3, 8.3	-22, 21	
f_{M6}		-5.4, 5.8	-16, 16	-32, 32	-1.3, 1.3
f_{M7}		-5.7, 6.0	-21, 20	-57, 56	-3.4, 3.4
f_{S0}		-5.7, 6.1			-2.7, 2.7
f_{S1}		-16, 17			-3.4, 3.4

Caution!
These are all
not unitarized
results!

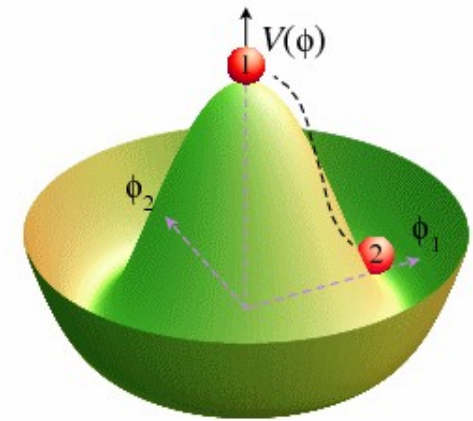


Study of VV polarizations in the final state

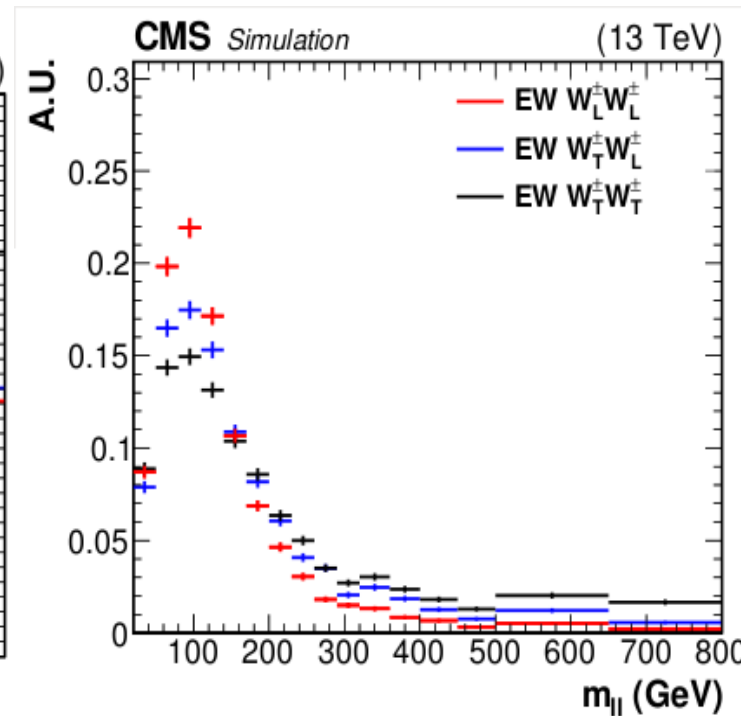
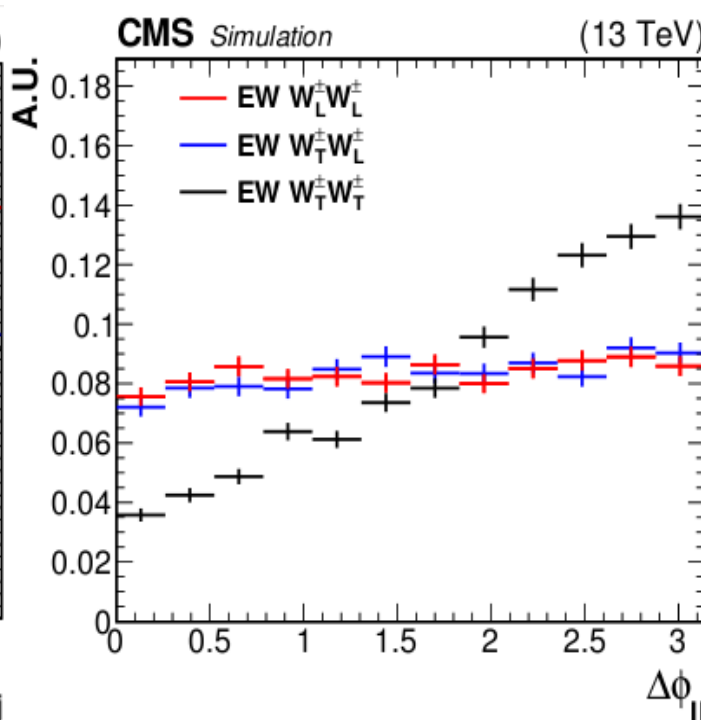
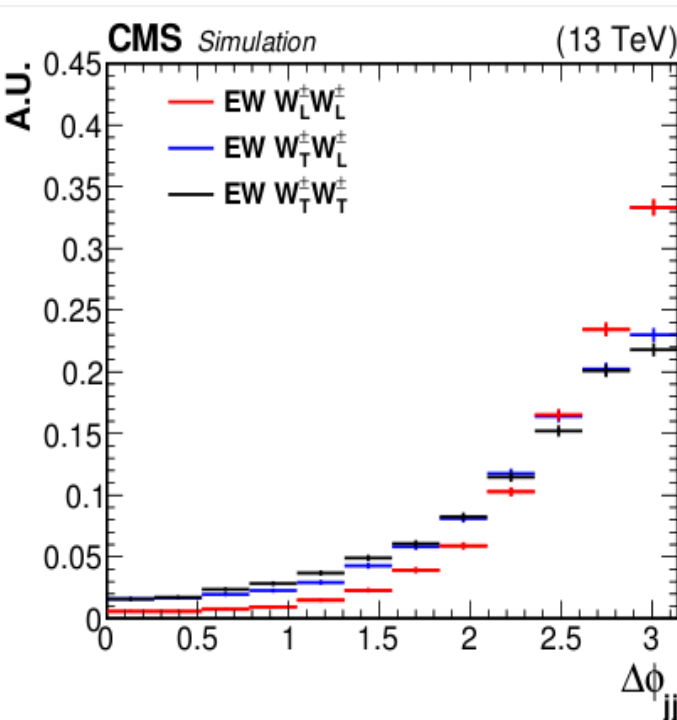
- Longitudinal modes are the most directly related to EWSB

$$\mathcal{L}_H = (D_\mu \phi)^\dagger (D^\mu \phi) - \mu^2 \phi^\dagger \phi - \lambda (\phi^\dagger \phi)^2$$

where $\phi = \begin{pmatrix} \phi^0 \\ \phi^- \end{pmatrix} = \frac{1}{\sqrt{2}} \begin{pmatrix} \phi_1 + i\phi_2 \\ \phi_3 + i\phi_4 \end{pmatrix}$



- But transverse modes are dominant in the data
- For a full multi-operator EFT analysis one needs to kinematically disentangle the effects of different operators



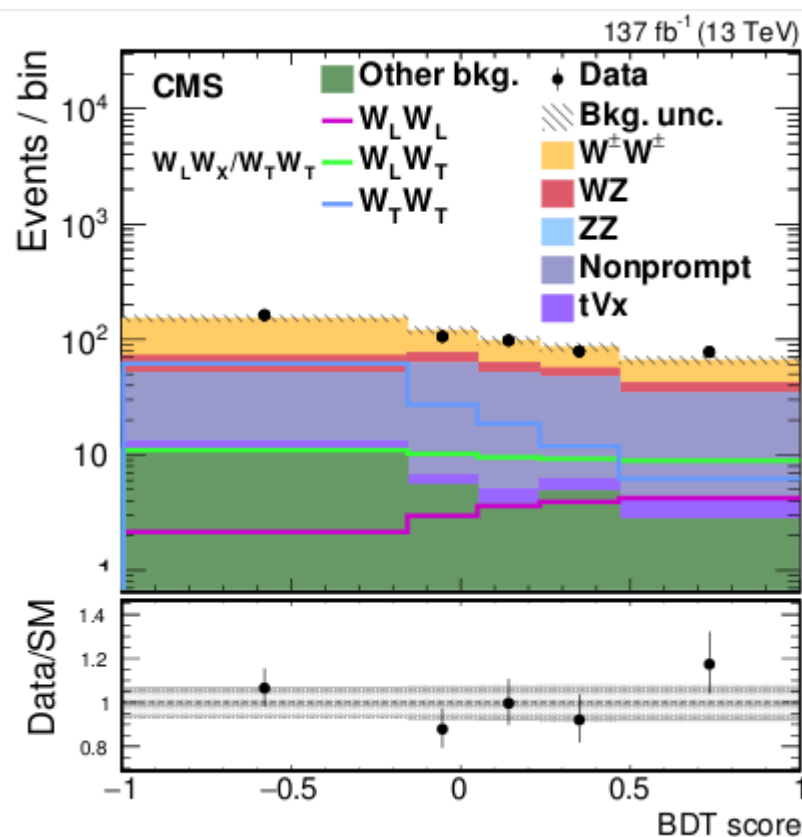
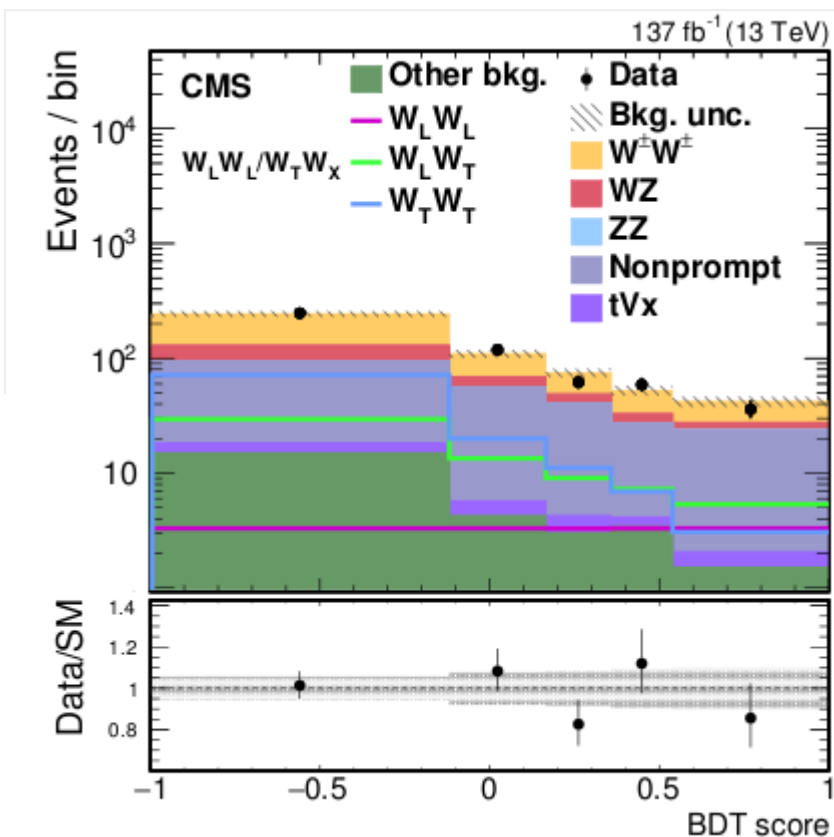
CMS: Polarizations in EW WWjj production

arXiv:2009.09429

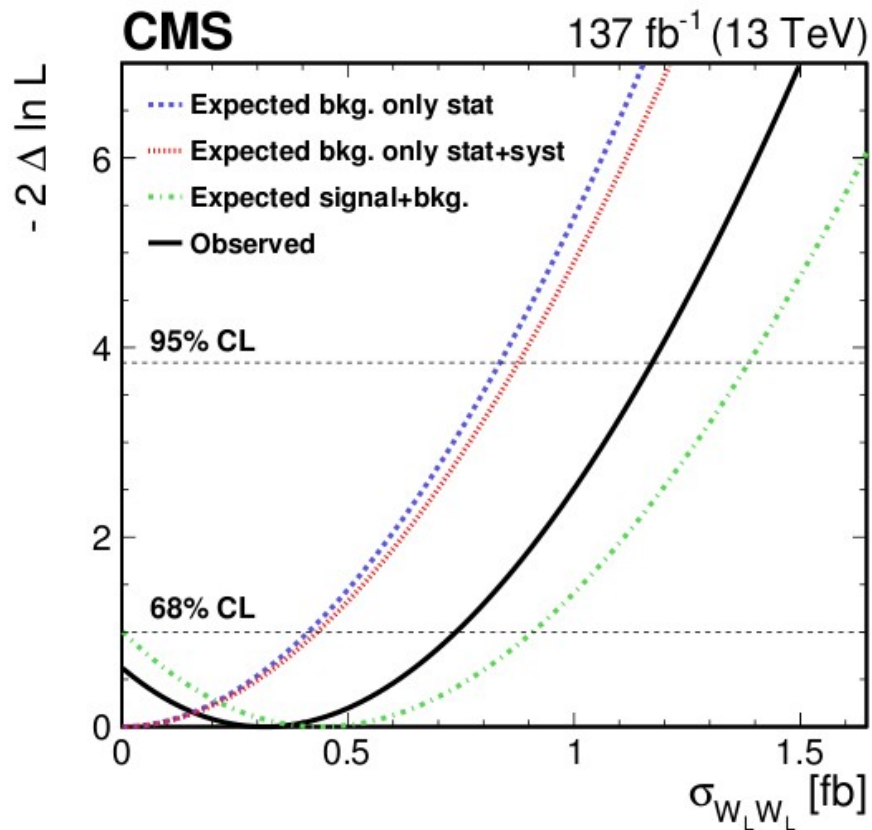
Same-sign WW process, fully leptonic

Analysis of Run II data (2016-2018), 137 fb⁻¹

- Two independent BDTs trained to distinguish $W_L W_L$ vs. $W_T W_X$ and $W_L W_X$ vs. $W_T W_T$ + an “inclusive” BDT to distinguish EW ssWW production from the SM background
- Polarization dependent templates fit to the data



Results: first experimental hint of longitudinal polarization



- Upper limits on $W_L W_L$ consistent with the SM

Helicity eigenstates defined in the WW c.o.m. frame

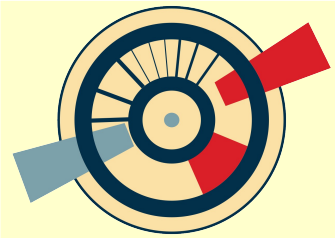
Process	$\sigma \mathcal{B}$ (fb)	Theoretical prediction (fb)
$W_L^\pm W_L^\pm$	$0.32^{+0.42}_{-0.40}$	0.44 ± 0.05
$W_X^\pm W_T^\pm$	$3.06^{+0.51}_{-0.48}$	3.13 ± 0.35
$W_L^\pm W_X^\pm$	$1.20^{+0.56}_{-0.53}$	1.63 ± 0.18
$W_T^\pm W_T^\pm$	$2.11^{+0.49}_{-0.47}$	1.94 ± 0.21

Hint of $W_L W_X$ at the level of 2.3σ
(SM expected: 3.1σ)

Helicity eigenstates defined in the parton-parton c.o.m. frame

Process	$\sigma \mathcal{B}$ (fb)	Theoretical prediction (fb)
$W_L^\pm W_L^\pm$	$0.24^{+0.40}_{-0.37}$	0.28 ± 0.03
$W_X^\pm W_T^\pm$	$3.25^{+0.50}_{-0.48}$	3.32 ± 0.37
$W_L^\pm W_X^\pm$	$1.40^{+0.60}_{-0.57}$	1.71 ± 0.19
$W_T^\pm W_T^\pm$	$2.03^{+0.51}_{-0.50}$	1.89 ± 0.21

Hint of $W_L W_X$ at the level of 2.6σ
(SM expected: 2.9σ)



Theoretical progress in defining polarization

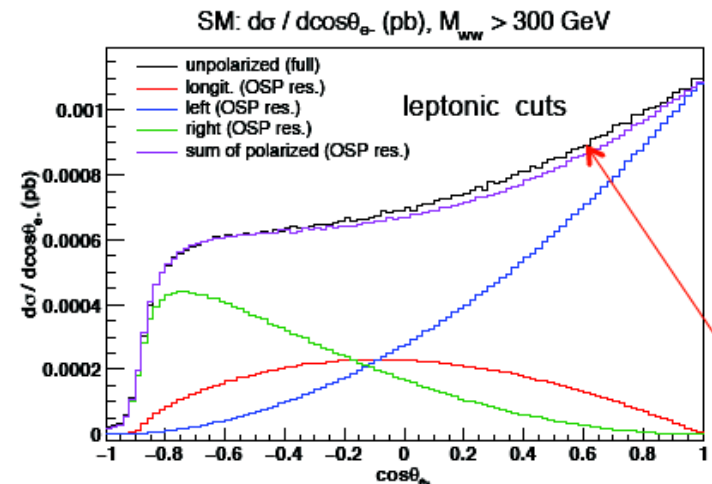
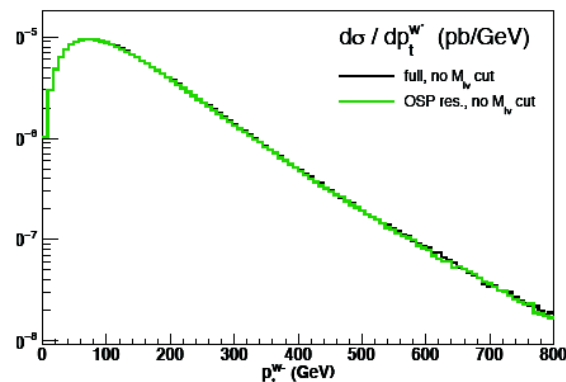
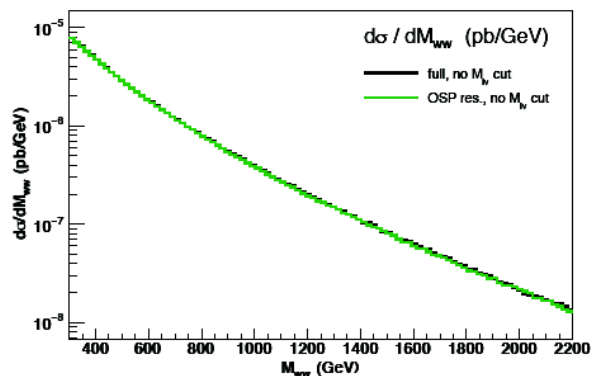
- Polarization is well defined for bosons on the mass shell. For off-shell interference present.
- Full pp process includes “non-resonant” diagrams (no intermediate VV).
- On-shell approximation (VV production x VV decay) good to ~5-10%.
- Novel idea (work by A. Ballestrero, E. Maina, et al.): ~2% agreement with full process

On shell projection (OSP)

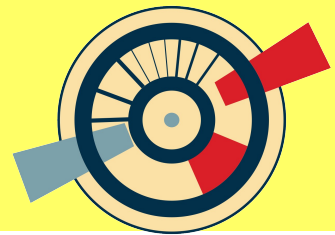
In computing the amplitudes of resonant contributions, one can project (in the numerator) the four momenta of the decay particles on shell

$$\mathcal{A}_f = \sum_{\lambda} \frac{\mathcal{A}_{p,RES}^{\mu}(p, k) \varepsilon_{\mu}^{\lambda} \varepsilon_{\nu}^{\lambda*} \mathcal{A}_d^{\nu}(k, q)}{k^2 - M_W^2 + i\Gamma_W M_W} + \mathcal{A}_{NONRES} \Rightarrow \sum_{\lambda} \frac{\mathcal{A}_{p,RES}^{\mu}(p, k_{OSP}) \varepsilon_{\mu,OSP}^{\lambda} \varepsilon_{\nu,OSP}^{\lambda*} \mathcal{A}_d^{\nu}(k_{OSP}, q_{OSP})}{k^2 - M_W^2 + i\Gamma_W M_W}$$

kind of On shell production X decay modulated by Breit Wigner



$p_t^e > 20 \text{ GeV}$, $|\eta^e| < 2.5$



BSM discovery in the EFT language

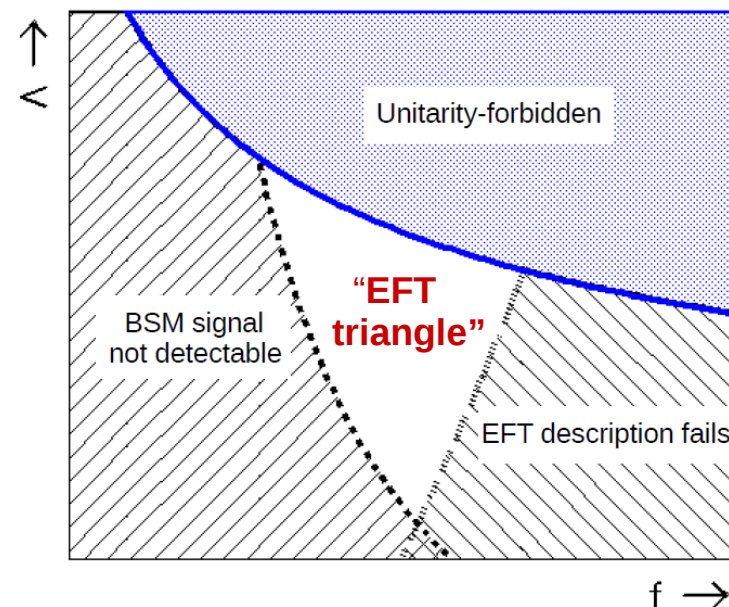
- $C = f \Lambda^4$, in models with one BSM scale and one BSM coupling, \sqrt{C} has the interpretation of the coupling constant (*Giudice et al. hep-ph/0703164*).

- **Master formula to normalize dim-8 operators for coupling constant extraction**

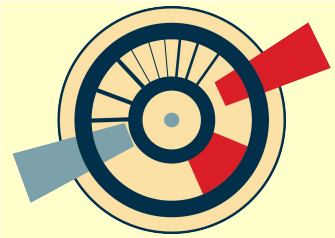
$$\frac{\Lambda^4}{16\pi^2} \left[\frac{\partial}{\Lambda} \right]^{N_p} \left[\frac{4\pi \phi}{\Lambda} \right]^{N_\phi} \left[\frac{4\pi A}{\Lambda} \right]^{N_A} \left[\frac{4\pi \psi}{\Lambda^{3/2}} \right]^{N_\psi} \left[\frac{g}{4\pi} \right]^{N_g} \left[\frac{y}{4\pi} \right]^{N_y}$$

(see arXiv:1601.07551)

- **Caveat: EFT description consistency requires the bulk of BSM signal originate from the EFT-controlled region (below Λ). Need to know M_{VV} .**
- **The inefficiency of the EFT to describe the data: 3 conditions – Unitarity vs. BSM discoverability vs. EFT consistency – largely at odds with each other. Only small “EFT triangles” are left** (see arXiv:1802.02366)

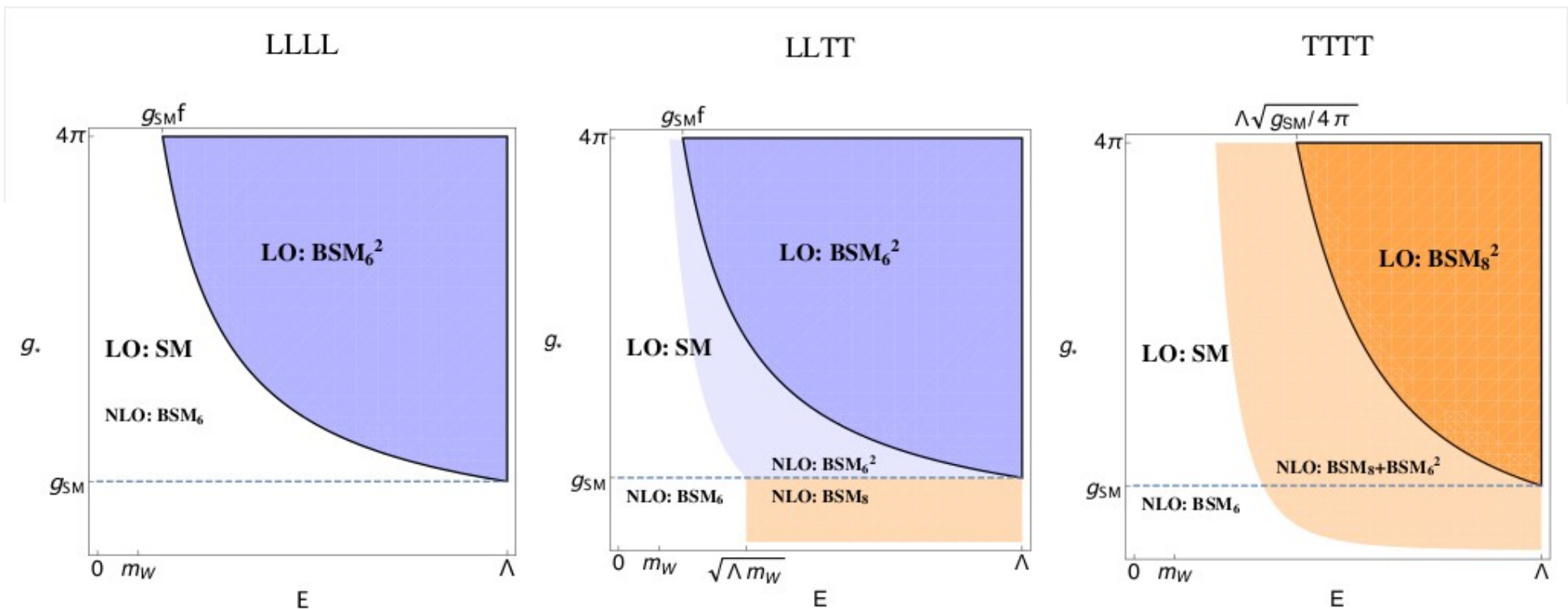


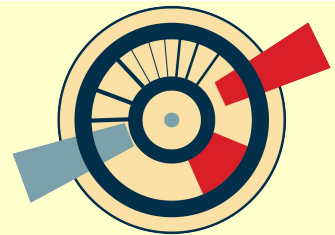
- **Combination of channels: simultaneous multi-operator fits to many processes. “Global fits” – so far focus on dim-6 only.**
- **The path to take: restricted global fits - VBS processes only and dim-8 operators + a handful of dim-6 for security, rest can be safely decoupled.**



Dim-6 vs dim-8 in VBS

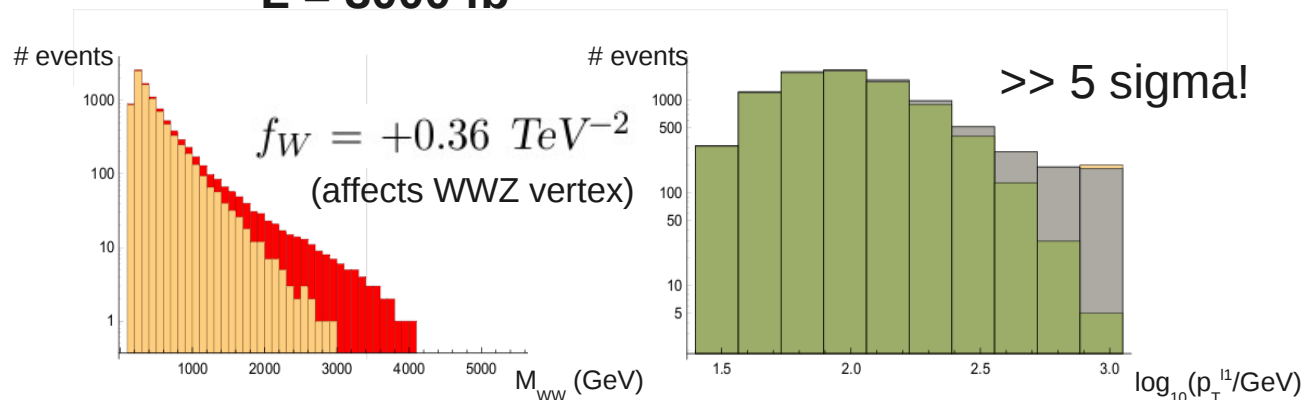
- Naively one expects dim-8 be a higher order correction to dim-6.
- But dim-6 contribution to VBS could be loop induced – additional factor $1/16\pi^2$ (hep-ph/9405214).
- Dim-8 can be indeed dominant in VBS in some BSM scenarios (arXiv:1607.05236).
- Full description of VBS requires both dim-6 and dim-8 terms.





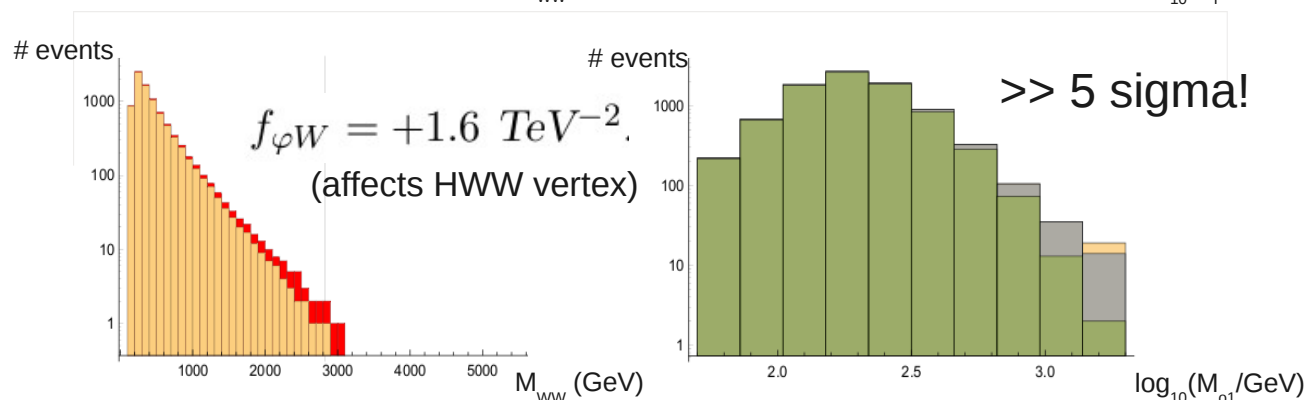
Potential impact of dim-6 operators on W+W+

L = 3000 fb⁻¹



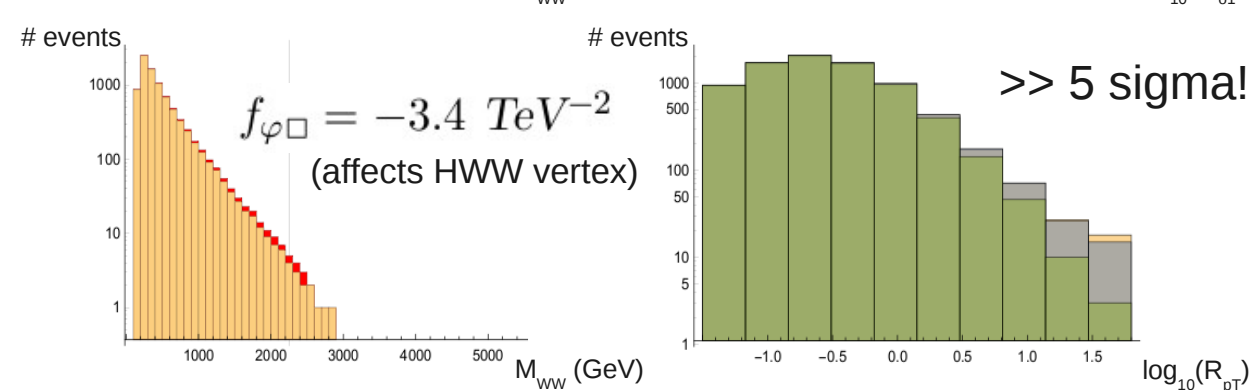
arXiv: 2011.07367

Some dim-6 operators within current experimental limits are not at all negligible when considered for a future VBS analysis at the HL-LHC



arXiv: 2101.03180

\mathcal{O}_W could be even further constrained by using VBS data already taken during Run 2



Summary and outlook

- VBS is an experimentally challenging, but very interesting theoretically, class of processes and a suitable place to look for possible deviations from the SM.
- VBS has been observed in Run 2 by both ATLAS and CMS in several different channels: $ssWW$, WZ , ZZ , $W\gamma$ and $Z\gamma$, in fully leptonic decay modes, at levels consistent with SM predictions.
- Semi-leptonic decay modes, although not permitting signal observation due to hadronic background, have been shown equally valuable in the search for physics BSM.
- First attempts to disentangle longitudinal polarization have been made, but we need more statistics for a conclusive observation.
- We are setting the path for a consistent, model independent search for BSM in the framework of Effective Field Theories; first results obtained using the “clipping” method are already available, more is in progress.
- Full description of VBS in the EFT language requires combination of dim-6 and dim-8 operators and a combination of channels.
- All the measurements are by far statistics-limited. We need more data.

Backup slides

Definitions and conventions

$$D_\mu \equiv \partial_\mu + i\frac{g'}{2}B_\mu + igW_\mu^i\frac{\tau^i}{2}$$

and the field strength tensors are

$$W_{\mu\nu} = \frac{i}{2}g\tau^i(\partial_\mu W_\nu^i - \partial_\nu W_\mu^i + g\epsilon_{ijk}W_\mu^jW_\nu^k),$$
$$\hat{W}_{\mu\nu} = \frac{1}{ig}W_{\mu\nu}. \quad B_{\mu\nu} = \frac{i}{2}g'(\partial_\mu B_\nu - \partial_\nu B_\mu)$$

for gauge fields W_μ^i and B_μ of $SU(2)_I$ and $U(1)_Y$, respectively.

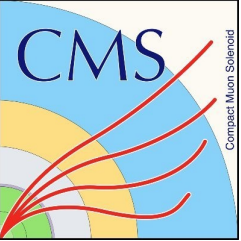
CMS: ssWW + WZ analysis

Table 2: Relative systematic uncertainties in the EW $W^\pm W^\pm$ and WZ cross section measurements in units of percent.

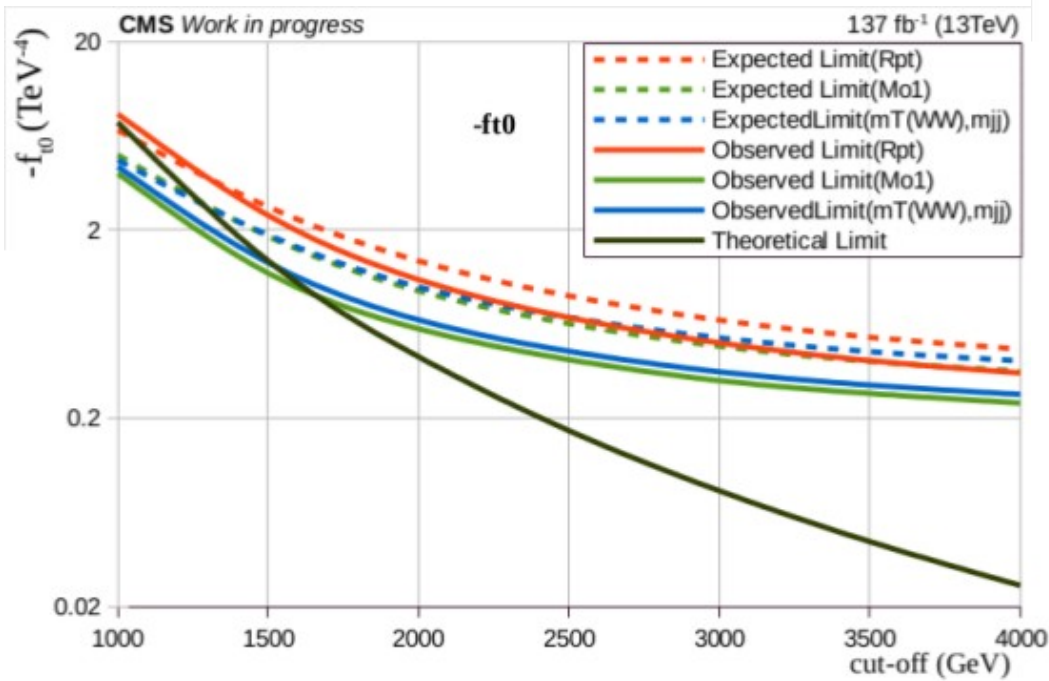
Source of uncertainty	$W^\pm W^\pm$ (%)	WZ (%)
Integrated luminosity	1.5	1.6
Lepton measurement	1.8	2.9
Jet energy scale and resolution	1.5	4.3
Pileup	0.1	0.4
b tagging	1.0	1.0
Nonprompt rate	3.5	1.4
Trigger	1.1	1.1
Limited sample size	2.6	3.7
Theory	1.9	3.8
Total systematic uncertainty	5.7	7.9
Statistical uncertainty	8.9	22
Total uncertainty	11	23

Table 3: List and description of all the input variables used in the BDT analysis for the WZ SR.

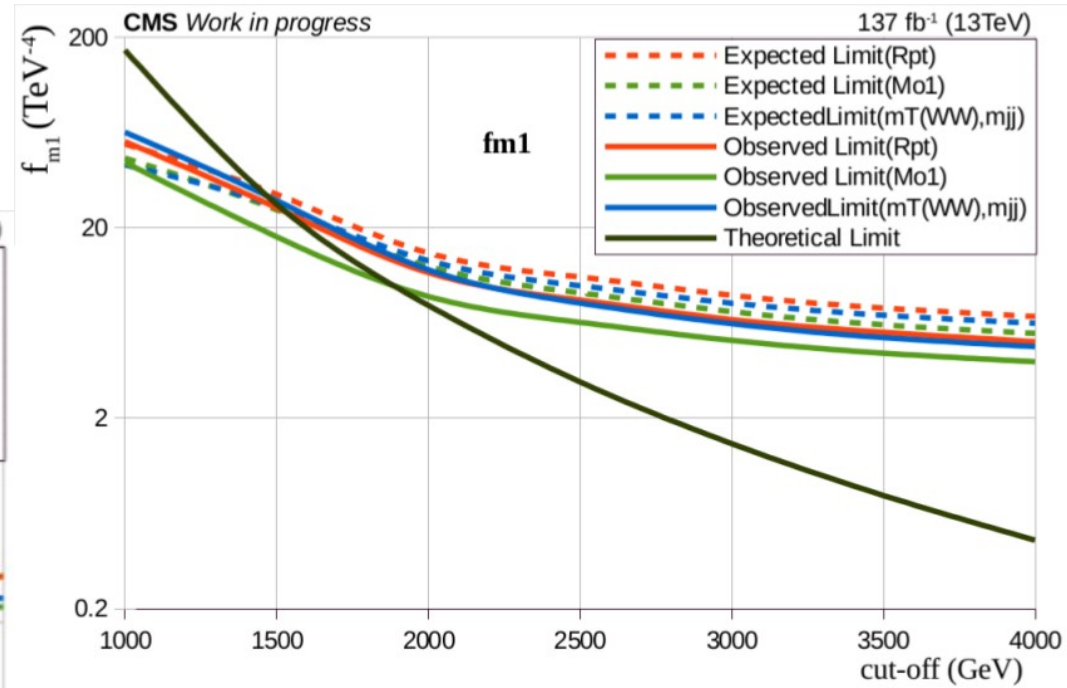
Variable	Definition
m_{jj}	Mass of the leading and trailing jets system
$ \Delta\eta_{jj} $	Absolute difference in rapidity of the leading and trailing jets
$\Delta\phi_{jj}$	Absolute difference in azimuthal angles of the leading and trailing jets
p_T^{j1}	p_T of the leading jet
p_T^{j2}	p_T of the trailing jet
η^{j1}	Pseudorapidity of the leading jet
$ \eta^W - \eta^Z $	Absolute difference between the rapidities of the Z boson and the charged lepton from the decay of the W boson
$z_{\ell_i}^*$ ($i = 1 - 3$)	Zeppenfeld variable of the three selected leptons
$z_{3\ell}^*$	Zeppenfeld variable of the vector sum of the three leptons
$\Delta R_{j1,Z}$	ΔR between the leading jet and the Z boson
$ \vec{p}_T^{\text{tot}} / \sum_i p_T^i$	Transverse component of the vector sum of the bosons and tagging jets momenta, normalized to their scalar p_T sum



"Full clipping" results – some more examples



f_{t0} – meaningful limits only for negative values



CMS: polarized ssWW analysis

Table 2: List and description of all the input variables for the signal BDT trainings.

Variables	Definitions
$\Delta\phi_{jj}$	Difference in azimuthal angle between the leading and subleading jets
p_T^{j1}	p_T of the leading jet
p_T^{j2}	p_T of the subleading jet
$p_T^{\ell_1}$	Leading lepton p_T
$p_T^{\ell_2}$	Subleading lepton p_T
$\Delta\phi_{\ell\ell}$	Difference in azimuthal angle between the two leptons
$m_{\ell\ell}$	Dilepton mass
$p_T^{\ell\ell}$	Dilepton p_T
m_T^{WW}	Transverse WW diboson mass
$z_{\ell_1}^*$	Zeppenfeld variable of the leading lepton
$z_{\ell_2}^*$	Zeppenfeld variable of the subleading lepton
$\Delta R_{j1,\ell\ell}$	ΔR between the leading jet and the dilepton system
$\Delta R_{j2,\ell\ell}$	ΔR between the subleading jet and the dilepton system
$(p_T^{\ell_1} p_T^{\ell_2}) / (p_T^{j1} p_T^{j2})$	Ratio of p_T products between leptons and jets
p_T^{miss}	Missing transverse momentum

Table 4: Systematic uncertainties of the $W_L^\pm W_L^\pm$ and $W_X^\pm W_T^\pm$, and $W_L^\pm W_X^\pm$ and $W_T^\pm W_T^\pm$ cross section measurements in units of percent.

Source of uncertainty	$W_L^\pm W_L^\pm$ (%)	$W_X^\pm W_T^\pm$ (%)	$W_L^\pm W_X^\pm$ (%)	$W_T^\pm W_T^\pm$ (%)
Integrated luminosity	3.2	1.8	1.9	1.8
Lepton measurement	3.6	1.9	2.5	1.8
Jet energy scale and resolution	11	2.9	2.5	1.1
Pileup	0.9	0.1	1.0	0.3
b tagging	1.1	1.2	1.4	1.1
Nonprompt lepton rate	17	2.7	9.3	1.6
Trigger	1.9	1.1	1.6	0.9
Limited sample size	38	3.9	14	5.7
Theory	6.8	2.3	4.0	2.3
Total systematic uncertainty	44	6.6	18	7.0
Statistical uncertainty	123	15	42	22
Total uncertainty	130	16	46	23